ELSEVIER

Review

# Reflections on small molecule manganese models that seek to mimic photosynthetic water oxidation chemistry

Christopher S. Mullins, Vincent L. Pecoraro *

*Department of Chemistry, The University of Michigan, 930 North University Avenue, Ann Arbor, MI 48109-1055, USA*

## Contents

## Abstract

Recent advances in the study of the oxygen evolving complex (OEC) of photosystem II (PSII) include structural information attained from several X-ray crystallographic (XRD) and spectroscopic (XANES and EXAFS) investigations. The possible structural features gleaned from these

studies have enabled synthetic chemists to design more accurate model complexes, which in turn, offer better insight into the possible pathways used by PSII to drive photosynthetic water oxidation catalysis. Mononuclear model compounds have been used to advance the knowledge base regarding the physical properties and reactivity of high-valent ($Mn^{IV}$ or $Mn^V$) complexes. Such investigations have been especially important in regard to the manganyl ($Mn^{IV}{=}O$ or $Mn^V(O)$) species, as there are no reports, to date, of any structurally characterized multinuclear model compounds that incorporate such a functionality. Dinuclear and trinuclear model compounds have also been thoroughly studied in attempts to draw further comparison to the physical properties observed in the natural system and to design systems of catalytic relevance. As the reactive center of the OEC has been shown to contain an oxo-$Mn_4Ca$ cluster, exact structural models necessitate a tetranuclear Mn core. The number of models that make use of $Mn_4$ clusters has risen substantially in recent years, and these models have provided evidence to support and refute certain mechanistic proposals. Further work is needed to adequately address the rationale for Ca (and Cl) in the OEC and to determine the sequence of events that lead to $O_2$ evolution.

## 1. Introduction

Nearly all of the dioxygen on our planet is produced photosynthetically by converting water to dioxygen. Thus, a full understanding of the mechanism of water oxidation by the oxygen evolving complex (OEC) of photosystem II (PSII) is significant not only to those in the field of chemistry, but also to the scientific community as a whole. The OEC is not an independent metalloprotein, but rather it is one component of the entire PSII protein complex. Photosynthetic organisms make use of a vast array of photopigments in the light harvesting region of PSII. Intermediary electron transfer residues (e.g. $Y_z$ and $Y_D$) are important for electron transfer directionality and cluster stability. The four electrons and four protons coupled to water oxidation are attained by the sequential oxidation of a $Mn_4Ca$ cluster. A chloride that is likely associated with this cluster is needed to carry out these reactions, but its function remains unknown. While structural clarity seems to be emerging for the $Mn_4Ca$ cluster, despite being intensively studied for many years, the mechanism of photosynthetic water oxidation remains a matter of contention amongst researchers.

It has been known since the early experiments by Joliet and Kok that four photon-induced charge separations drive transitions between five oxidation levels named $S_0$–$S_4$ [1–4]. The $S_0$ state is the most reduced enzymatic form and is unstable with respect to oxidation by $Y_z^+$ to give $S_1$, which is the dark stable resting state. The most oxidized species, $S_4$, is also unstable, releasing $O_2$ and regenerating $S_0$. The chemical identities (structure) of the "reactive" $S_4$ state, and the $S_0$ "product" state are critical to gaining a more complete understanding of the mechanism of photosynthetic water oxidation. Numerous mechanisms have been put forth for water oxidation by the OEC. Undoubtedly, many of these will be discussed at length in other portions of this issue. Instead, we will focus on our preferred mechanistic description: the nucleophilic attack by a water or hydroxide coordinated to either manganese, or more likely, calcium, on an electrophilic manganyl species, to form the O–O bond. However, before discussing this mechanism in detail, we must first set the stage by understanding key structural, spectroscopic, and kinetic studies. This chapter will emphasize the role of small molecule models in the development of ideas for water oxidation.

Over the past 30 years, numerous compounds have been touted as some form of model for the OEC. The structures and physical properties of many of these complexes have been previously analyzed in numerous reviews to which the interested reader is referred [5–15]. Herein, emphasis will be given to less recognized structures that may now be more relevant to understanding water oxidation chemistry. This review was first written in March 2007 and revised in July of the same year.

## 2. Structural biology of the OEC in the new millennium

Recently, several X-ray crystallographic studies of this enzyme have revealed possible structural features. The recent crystallographic study by Barber and coworkers at 3.5 Å resolution (Fig. 1a) reveals a $Mn_3CaO_4$ cubane linked to a dangler Mn atom [16,17] in which the Mn and Ca are principally coordinated by oxo and carboxylate donors. While the more recent structure of Zouni and coworkers (3.0 Å) does not pinpoint the bridging oxygen atoms in the cluster it does offer better overall crystallographic resolution [18]. Other differences between the two structures relate to the spatial distribution of the metal ions and mode of ligation of the nearby amino acid residues.

Although the X-ray crystal structures have significantly enhanced the understanding of the structure of the OEC, they also have been controversial. The problem is that metal ion reduction may occur during data collection [19]. In order to circumvent this problem, Yachandra and coworkers have conducted oriented EXAFS experiments to ascertain the actual geometry of the $Mn_4Ca$ cluster [20]. This technique offers two distinct advantages: lower intensity radiation and the ability to orient the metals with respect to the membrane. By using lower X-ray doses in the EXAFS experiments the authors suggest that it is possible to avoid reduction of the manganese atoms in the OEC and still allow for measurement of metal–metal distances. The analysis still relies on knowledge of the crystallographic coordinates, but provides an alternative way of looking at the manganese cluster. Three models were found to be compatible with the polarized Mn EXAFS spectra of single crystals of PSII. From these three models, the authors chose to highlight the ligand environment for the best-fit orientation of the structural representation shown in Fig. 1b. While there are slight modifications of the structure as compared with the crystallographic models, one can still think of the system as an $Mn_4Ca$ cluster with one Mn ion distinct from the other three.
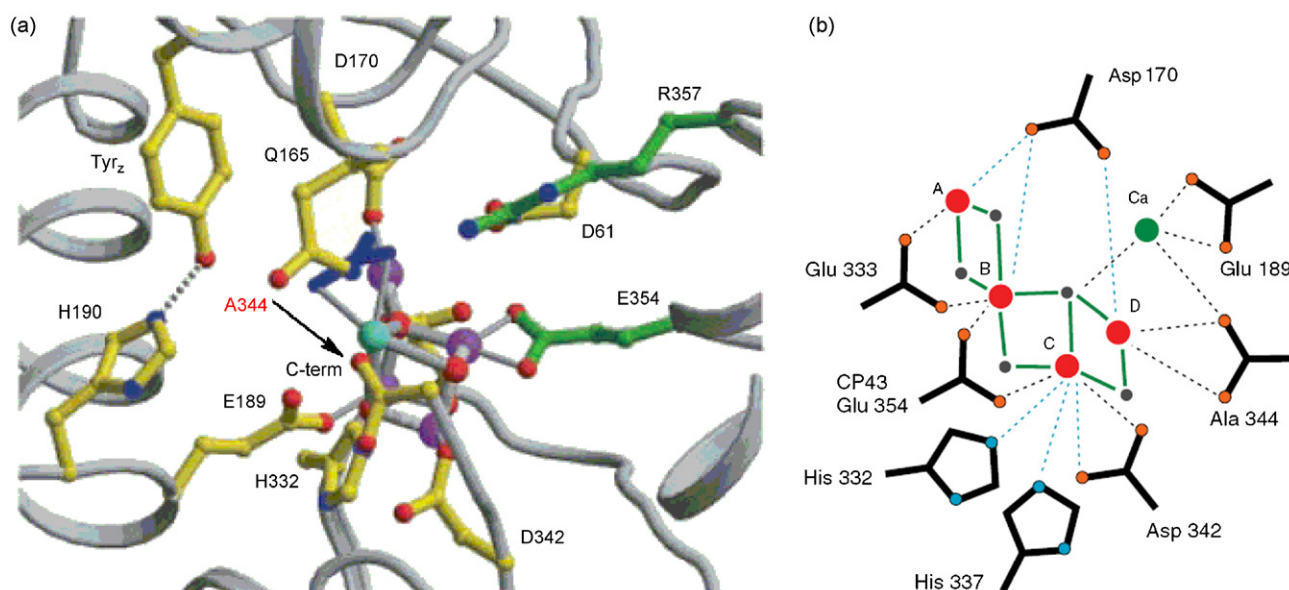
Fig. 1. Two proposed structures for the OEC of PSII. (a) View of the reaction center based on the 3.5 Å crystal structure model of the OEC, pdb 1S5L (figure was reproduced from Ref. [16], with permission from AAAS) and (b) one of three proposed structures for the OEC as determined by polarized Mn EXAFS spectroscopy (figure was reproduced from Ref. [20], with permission from AAAS).

## 3. Structural models of the OEC

### 3.1. Mononuclear Mn complexes

#### 3.1.1. Non-manganyl

While it is known that the OEC consists of a tetranuclear cluster of Mn ions that cycle through the various S-states during the water oxidation process, mononuclear models are useful in that they provide relatively straightforward syntheses for the isolation of high-valent complexes. Despite the proposition that $Mn^V$ may be an important component of $S_4$, there are currently no examples of small molecule model complexes containing $Mn^V$ as dinuclear or higher nuclearity structures that have been crystallographically characterized. Furthermore, given the 3 + 1 cluster formulation, mononuclear complexes may reveal interesting properties for the "dangler" Mn atom. Investigations into mononuclear Mn systems in the $Mn^{IV}$ and $Mn^V$ oxidation states have enabled the examination of spectroscopic features for comparison with those observed in the OEC. Included in this class of compounds are simple $Mn^{IV}$ monomers and complexes that contain a terminal manganyl, or Mn-oxo species.

The first structurally characterized mononuclear $Mn^{IV}$ complexes were reported independently by Christou and coworkers [21] and Pecoraro and coworkers [22,23] in the late 1980s. Christou and coworkers reported the synthesis of the mononuclear complex, $[Mn^{IV}(sal)_2(bipy)]$ (sal = salicylicate, bipy = 2,2′-bipyridine), **1**, from the ligand substitution reaction of NaHsal with the mixed-valent $[Mn_2O_2(bipy)_4](ClO_4)_3$ complex [21]. The metal oxidation assignment was verified by the Evans NMR method to determine the value of $3.83\mu_B$ for the solution magnetic moment, which is consistent with a $d^3$ $Mn^{IV}$ center. At about the same time, Pecoraro reported several $Mn^{IV}$ Schiff base complexes with $N_2O_4$ ligation [22,23]. The mononuclear complex $Mn^{IV}(saladhp)_2$ (saladhp = 2-salicylideneiminato-1,3-dihydroxy-2-methylpropane) had a comparable magnetic moment (solid-state value of $3.91\mu_B$), however, this complex was found to have a redox stability of nearly 900 mV compared with **1** [22]. More recently, Pecoraro and coworkers have reported a series of $Mn^{IV}N_2O_4$ complexes (e.g. **2**), which show the range of redox potentials that can be sampled with the same first coordination sphere ligands [24]. These types of compounds were also critical to the understanding of $Mn^{IV}$ in biology as they provided the first detailed EPR spectral evaluation of $Mn^{IV}$. Another key finding from these studies was that $Mn^{IV}$ is often not strongly oxidizing, as was previously thought to be the case. Wieghardt and coworkers established that phenolate ligands are often non-innocent with higher metal oxidation states [25]. However, in the case of complex **2** reported by Pecoraro, the phenolate ligands may be regarded as innocent. Of greatest interest are the strong EPR spectral features exhibited by **2** in the $g = 2$ region with only minor components at $g = 4.1$, unlike other reported $Mn^{IV}N_2O_4$ compounds (Fig. 2).

During the mid-1980s, a significant controversy developed regarding the nuclearity of the OEC cluster. At question was whether all four manganese were associated with a single cluster or if there was a mononuclear site at some distance from the main manganese cluster [26]. To resolve this issue, it became important to understand the EPR spectroscopy of mononuclear Mn centers. The EPR spectra of $d^3$ $Mn^{IV}$ and $Cr^{III}$ ions in an axial field ($E/D = 0$) are often difficult to interpret as they greatly depend on the magnitude of the zero-field splitting (zfs) parameters [27–29]. A simplification may be achieved when the axial zfs parameter $D$ is either much greater than the applied microwave frequency ($2D \gg h\nu$) or much smaller than ($2D \ll h\nu$) ($h\nu \approx 0.31\,cm^{-1}$ at X-band frequencies). When the value for $D$ is large, a strong signal is found at low field along with a weaker $g = 2$ component. Such is the case for $Mn^{IV}$ complexes with hard oxygen-rich catecholato [30] and sorbitalato [31] lig-
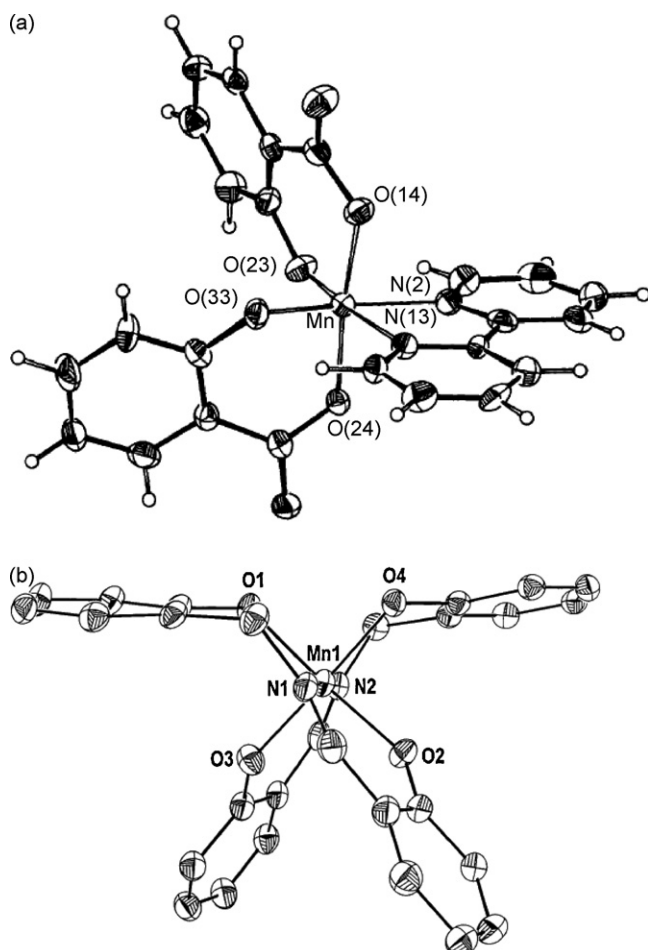
Fig. 2. ORTEP representations for the mononuclear $Mn^{IV}N_2O_4$ model complexes: (a) $[Mn^{IV}(sal)_2(bipy)]$, **1** (figure was reproduced from Ref. [21], by permission of The Royal Society of Chemistry) and (b) $[Mn^{IV}(dbpip)_2]$, **2** (butyl groups are removed for clarity) (figure was reproduced from Ref. [24], with permission of copyright holders Elsevier (2002)).



Fig. 3. EPR spectra of $Mn^{IV}N_2O_4$ model complexes: (A) $Mn(SALAHP)_2$ [23] in DMF/MeOH(3:2) at 100 K; (B) $Mn(als)_2$ [33] in dichloromethane/toluene (1:1) at 77 K; (C) complex **2**, $[Mn^{IV}(dbpip)_2]$, in dichloromethane at 4 K [24] (this figure was reproduced from Ref. [24], with permission of copyright holders Elsevier (2002)).

ands. In the latter instance, where $D$ is small, the $g = 2$ signal dominates with relatively weak low field signals. This is seen for sulfur-containing thiohydroxamato [28] and dithiocarbamato [32] manganese(IV) complexes. The EPR spectra become isotropic when the extreme limit of $D = 0$ exhibiting a strong signal at $g = 2$.

There are several examples of $Mn^{IV}N_2O_4$ complexes which have two chelating dianionic, tridentate Schiff base ligands, composed of one imine nitrogen, one phenolate oxygen, and one alkoxide oxygen donor to form a neutral octahedral complex. The EPR spectra of several $Mn^{IV}N_2O_4$ model complexes are compared in Fig. 3. These complexes, which have two alkoxide donors bound to Mn, exhibit hyperfine coupling on two well-resolved low-field features [22,23]. Such compounds do not fall within the axial approximation as they have $E/D$ values $\approx 0.22$. In a related series reported by Chakravorty and coworkers [33], the two phenolates found in **2** are substituted by carboxylate groups. This relatively minor change has a profound effect on the EPR spectrum (Fig. 3B). The low field feature loses its hyperfine resolution and the weaker component disappears. Such a spectrum is typical of a species with $D \gg 0.33 \, cm^{-1}$. The EPR spectrum
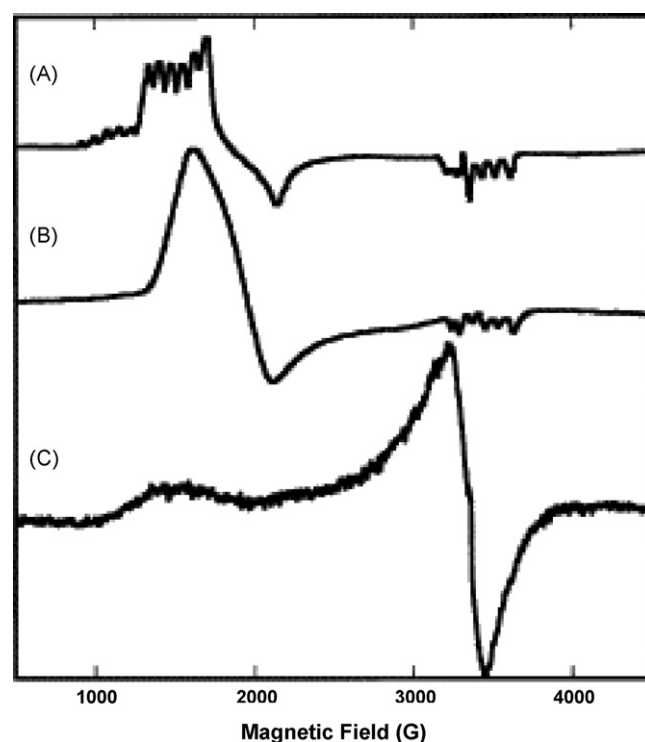
of **2** (Fig. 3C) bears no resemblance to any of the previously reported $N_2O_4$ spectra. Here, the $D \ll 0.31 \, cm^{-1}$ axial limit is approached.

In 2006, Busch and coworkers reported the structure of $[Mn^{IV}(Me_2EBC)(OH)_2](PF_6)_2$, **3** (Fig. 4, left) which was proposed to be the first structurally characterized example of a mononuclear $Mn^{IV}$ complex with terminal hydroxo ligands [34]. Such compounds are important for understanding possible substrate interactions with Mn in the higher S-states. A $Mn^{IV}$ complex with a terminal hydroxo ligand was reported as early as 1968, but no crystallographic data was available to substantiate this claim [35]. The pH titration of aqueous solutions of **3** revealed two acid–base equilibria with $pK_{a1} = 6.86$ and $pK_{a2} = \sim 10$, the latter apparently being associated with dimer formation. More recent work with this complex has revealed its catalytic features with respect to olefin epoxidation and hydrogen atom abstraction [36,37]. Bond dissociation energy (BDE) calculations were used to compare reduced forms of the two oxidizing species: $[Mn^{III}(Me_2EBC)(OH)(H_2O)]^{2+}$, $BDE_{OH} \approx 83.0 \, kcal/mol$ and $[Mn^{III}(Me_2EBC)(OH)_2]^+$, $BDE_{OH} \approx 84.3 \, kcal/mol$. The similar magnitude of these two values was taken to indicate that the H-atom abstracting abilities of $Mn^{IV}=O$ and $Mn^{IV}–OH$ are thermodynamically very similar, despite their difference in charge and abstracting functional group [37]. These HBDE's stand in contrast to the higher values reported by Borovik for other mononuclear $Mn^{IV}$ species (*vide infra*).
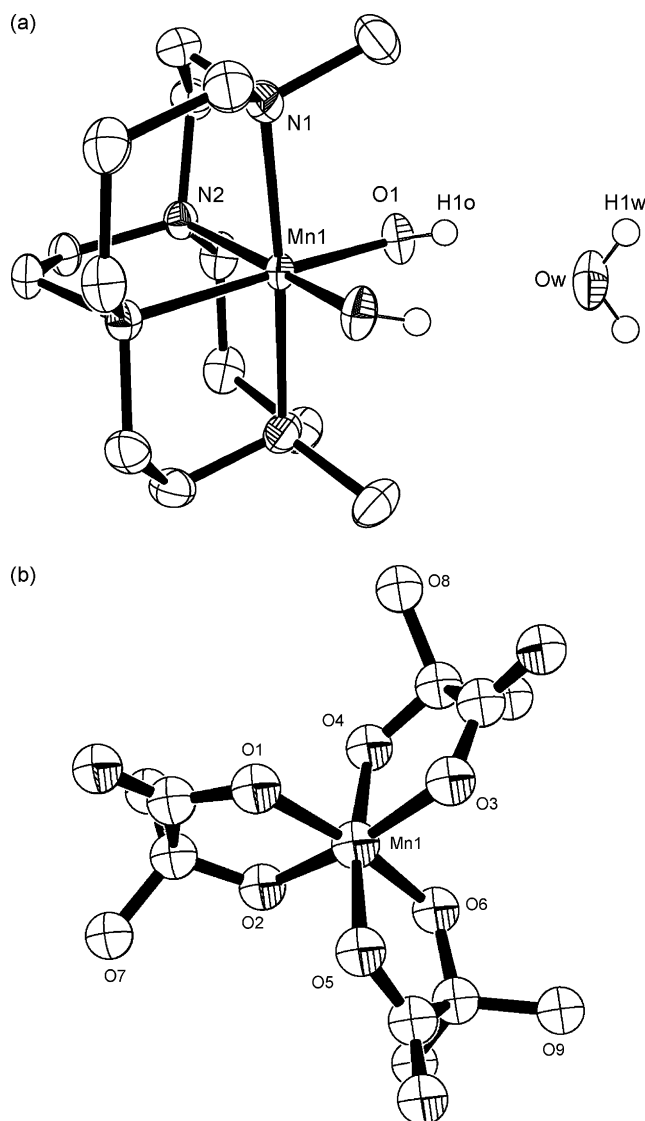
(a)



(b)



Fig. 4. ORTEP representations for mononuclear Mn$^{IV}$ bis-OH complex reported by Busch and coworkers, **3** (figure was reproduced from Ref. [34], Copyright (2006) American Chemical Society) and the Mn$^{IV}$O$_6$ complex reported by Saadeh and Pecoraro, **4** (figure was reproduced from Ref. [38], Copyright (1991) American Chemical Society).

Saadeh and Pecoraro reported the X-ray structure of Na$_3$[NaMn$_2^{IV}$(HIB)$_6$]·4MeOH, **4**, which revealed a mixed-metal trinuclear cluster composed of two Mn$^{IV}$ octahedra bridged by a sodium ion [38]. The face-shared geometry, shown in Fig. 4, left, leads to a very short Mn–Na distance (2.98 Å). Complex **4** is a unique Mn$^{IV}$ complex with all oxygen ligation and containing redox-innocent ligands [38]. A thorough comparison of known mononuclear Mn$^{IV}$ complexes in several coordination environments was carried out to evaluate the hypothesis of Hansson et al. [26] that the signal at $g = 4.1$ observed in S$_2$ arises from an isolated mononuclear center. This model has been challenged on grounds that the low-field signals of mononuclear Mn$^{IV}$ will show $^{55}$Mn hyperfine coupling, that the signals should be absorptive rather than derivative shaped, and that they will not give $g_{eff}$ values at $g \approx 4.1$. Through detailed

studies of numerous mononuclear Mn$^{IV}$ complexes it became clear that the $g = 4.1$ signal was not due to a mononuclear center [39]. This point was ultimately proven by Klein when a multiline feature was observed on this low-field signal after PSII preparations were treated with ammonia [40].

### 3.1.2. Manganyl

The first reported structurally characterized manganyl complex was [Mn$^V$=O(HMPAB)]$^-$, **5** [41]. The H$_4$HMPAB ligand (1,2-bis(2-hydroxy-2-methylpropanamido)benzene) was designed by Collins and coworkers to be an oxidation-resistant tetradentate amidate ligand [42]. The manganyl complex was synthesized by the reaction of [Mn$^{III}$(HMPAB)]$^-$ with excess *t*-butyl hydroperoxide to give **5** (Fig. 5, left). The reported Mn-oxo bond length of 1.548(4) Å, suggests significant triple bond character [41]. Also of note are the interactions between the Na ion and the alcoholic oxygen atoms (2.339(4) and 2.370(4)) which represent a bridge between the metal ions. A year later, Collins reported a water-soluble Mn$^V$-oxo complex, **6** (Fig. 5, center) derived from a macrocyclic tetraamidate ligand [43]. The Mn–O bond length herein was 1.555(4) Å, again indicative of triple bond character. The oxo ligand was reported to exchange in $^{18}$O-labeled water, permitting the first assignment of a $\nu$(Mn–O) infrared vibration, which were found as: $^{16}$O-labeled, 979 cm$^{-1}$; $^{18}$O-labeled, 942 cm$^{-1}$.

A more recent adaptation of the tetraamido ligand framework incorporated a pyridine ring (where a benzene ring was utilized previously) as the linkage between two of the amide functionalities [44]. The structure of the complex anion, **7**, is illustrated in Fig. 5, right. This minor adjustment in the ligand backbone enabled cation binding, as shown by UV–vis titration experiments. Collins proposed that secondary ion binding would lead to an increase in the electrophilic character of the Mn-oxo group, and in turn, further activate such complexes toward O-atom transfer chemistry.

These complexes are good structural models for understanding the spectroscopic features of manganyl functionalities that may be present in the latter S-states. Manganyl complexes have also garnered substantial attention as proposed reactive intermediates in asymmetric olefin epoxidation [45–47]. Collins and coworkers have employed these oxidation-resistant ligands for a number of green oxidation catalysts for industrial waste and other environmental problems [44,48].

Despite the fact that these manganyl complexes have not been shown to be useful water oxidation catalysts, the compounds developed by Collins have been quite useful to our understanding of biological water oxidation. A seminal paper by Babcock proposed that a manganyl was formed in S$_3$ [226]. In 2004, the XANES spectrum of complex **5** was reported by Pecoraro and coworkers in order to test Babcock's mechanism. It was shown that strongly $\pi$-bonded oxo ligands increase the allowedness of the 1s → 3d pre-edge transitions significantly. Thus, XANES spectroscopy can detect even small amounts of transiently formed Mn=O compounds [49]. By comparing the authentic Mn$^V$-oxo with the pure S$_3$ state, it was clearly shown that a manganyl is not present S$_3$. This fact is illustrated in Fig. 6, which shows a comparison of the XANES spectra for various
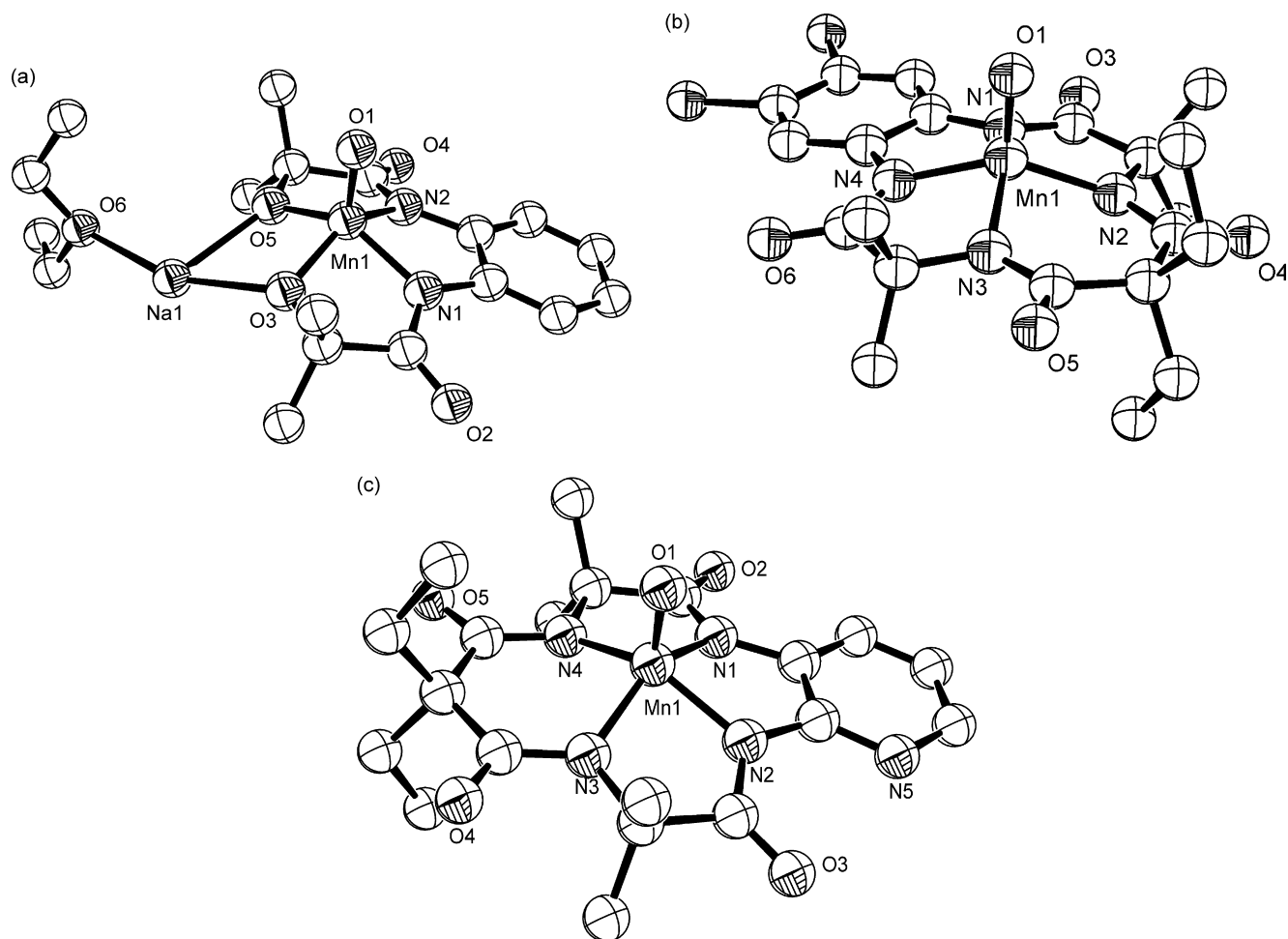
Fig. 5. ORTEP representations for the mononuclear Mn$^V$(O model complexes reported by Collins and coworkers: (a) **5** (figure was reproduced from Ref. [34], Copyright (1989) American Chemical Society), (b) **6** (figure was reproduced from Ref. [43], Copyright (1990) American Chemical Society), and (c) **7** (figure was reproduced from Ref. [44], Copyright (1998) American Chemical Society).
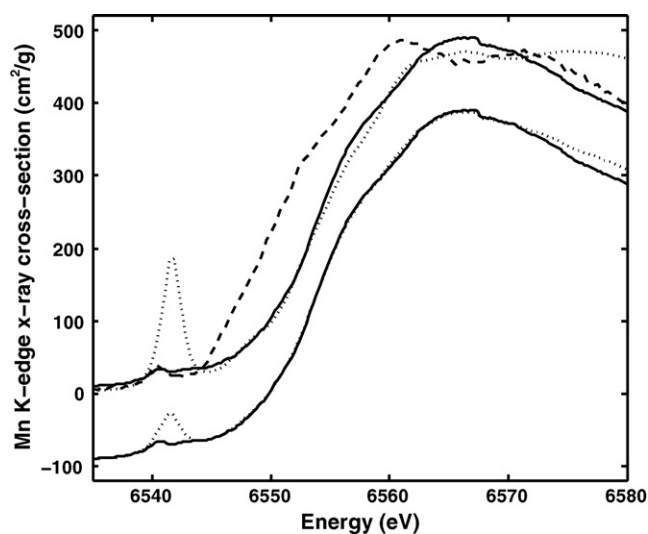


Fig. 6. (Top) XANES spectra for **5**, Na[Mn$^V$(O(HMPAB)] (dotted line), (Na[Mn$^{III}$(HMPAB)(EtOH)$_2$]) (dashed line), and **8**, [Mn$_2$$^{IV}$(2-OH-3,5-di-(*t*-Bu-salpn)](NO$_3$)$_2$ (solid line). (Bottom) Simulated XANES for a hypothetical Mn$_3$$^{IV}$Mn$^V$(O (dotted line) and authentic [Mn$_2$$^{IV}$(2-OH-3,5-di-(*t*-Bu-salpn)](NO$_3$)$_2$, (**8**, solid line) structures (figure was reproduced from Ref. [49], Copyright (2004) American Chemical Society).

models along with the S$_3$ state. This experiment was the critical study to discount the Babcock mechanism or any other proposal that invokes a manganyl at S$_3$ of the Kok cycle. A year later, Dau used this observation to conclude that a manganyl species does not exist immediately after illumination to yield S$_4$ [227]. Unfortunately, one still cannot evaluate the existence of manganyl in a possible S$_4'$ state of the cycle.

O'Halloran and coworkers reported the only other crystallographically characterized Mn$^V$-oxo species in 1994 [50]. An ORTEP representation of complex **9** is provided in Fig. 7. The ligand bears striking resemblance to the original complex reported by Collins, albeit with a more sterically demanding ligand architecture. Unlike the Collins compounds, which are prepared by the reaction of Mn$^{III}$ salts and alkyl peroxides, this Mn$^V$=O complex was prepared by a direct reaction with dioxygen. In this complex, the reported Mn-oxo bond length was insignificantly lengthened to 1.558(4) Å, thus keeping it in the range of a formal Mn–O triple bond. The stability of these complexes is thought to result from significant overlap between the metal d and oxo ligand p orbitals [51]. Typically, the Mn$^V$-oxo complexes that are isolable are also too stabilized and display little, if any, chemical reactivity related to the OEC.
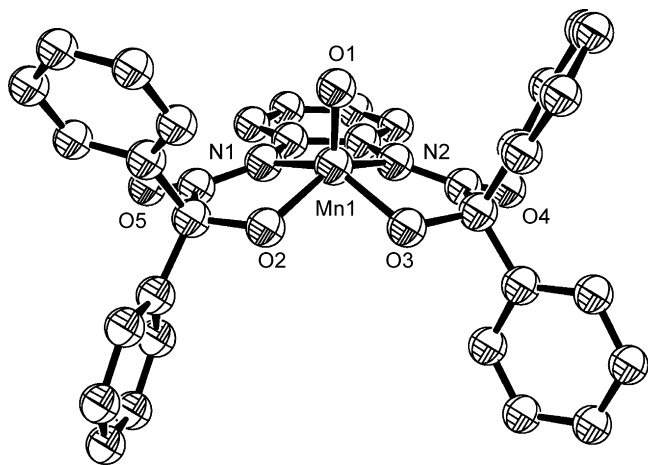
Fig. 7. ORTEP representation for the mononuclear Mn$^V$-oxo model complex, **9**, reported by O'Halloran and coworkers (figure was reproduced from Ref. [50], Copyright (1994) American Chemical Society).



Fig. 8. (a) Normalized Mn XANES spectra for [(TBP$_8$Cz)Mn$^{III}$(MeOH)] (dashed line) and [(TBP$_8$Cz)Mn$^V$(O)], **10** (solid line); (b) ORTEP diagram of [(TBP$_8$Cz)Mn$^{III}$(MeOH)], **11** (the *tert*-butyl phenyl substituents are not shown for clarity) (figure was reproduced from Ref. [52], Copyright (2005) American Chemical Society).

More recently, Goldberg and coworkers reported the XANES spectrum for a putative Mn$^V$=O species derived from a Mn$^{III}$-corrolazine complex [52]. Although the crystal structure of the manganyl complex has yet to be determined, the XANES spectrum (Fig. 8a) for [(TBP$_8$Cz)Mn$^V$(O)], **10**, provides the basis for assignment as a Mn$^V$-oxo species due to the intense pre-edge feature near 6541 eV that is typical for such systems. The best fit of the EXAFS data gives a short Mn–O bond distance of 1.56 Å, confirming the structure of the manganyl unit in **10**. This bond distance falls in line with those observed from XRD studies of other Mn$^V$-oxo complexes in which the metal-oxo bond has significant triple-bond character. Detailed spectro-electrochemical studies of **10** and **11** (structure shown in Fig. 8b) revealed multiple, reversible redox processes for both complexes including a relatively low potential for the Mn$^{IV/V}$ couple in **9** (near 0.0 V versus SCE). Chemical reduction of **10** results in the formation of a Mn$^{III}$Mn$^{IV}$(μ-O) dimer as characterized by EPR spectroscopy [52].

The Jacobsen/Katsuki olefin epoxidation catalysts, which are Mn$^{III}$ salen complexes (H$_2$salen = bis(salicylidene) ethylenediamine), are well established and known to proceed with a wide range of substrates affording products with very high enantioselectives [53–59]. Despite the considerable synthetic importance of these systems and the numerous mechanistic investigations, very little is known about the exact method of oxygen transfer. Furthermore, the identity of the actual catalytic species remains controversial [54,60–65]. Most mechanistic models involve a reactive [Mn$^V$-oxo(salen)] complex [66]. Generally it is assumed that this oxomanganese complex is the reaction product of the Mn$^{III}$ salen and the oxidant (e.g. 3-chloroperoxybenzoic acid (*m*-CPBA)), followed by oxygen atom transfer to the olefin either in a stepwise radical process [67,68] or via a metallaoxetane [69–73]. Alternatively, the Mn$^V$-oxo species can be formed by the disproportionation of a bis(μ-oxo)Mn$^{IV}$ dimer [74]. To date, the most compelling evidence for a manganyl species stems from ESI-MS studies [75,76].

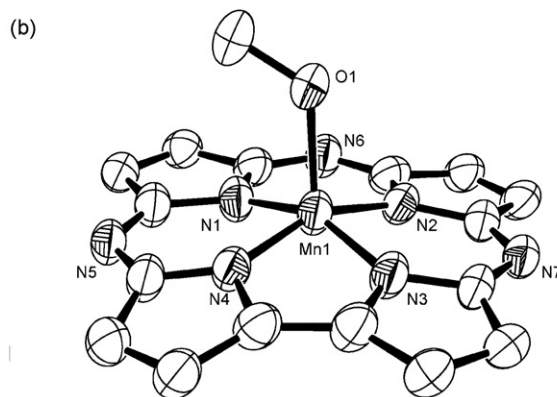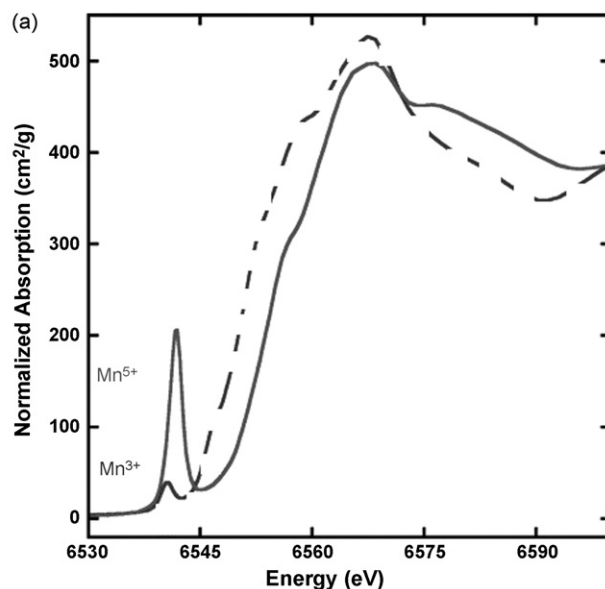Recently, Feth and coworkers used various spectroscopic handles to establish the identity of the high-valent manganese intermediates derived from the reaction of Mn$^{III}$ salen complexes and oxidants in solution [66]. Their results suggested that neither a μ-oxo dimeric structure nor a Mn$^V$-oxo species is formed upon oxidation with *m*-CPBA. The reasons provided for ruling out a manganyl species were: (1) the lack of Mn–O distance in the range of 1.5 → 1.6 Å in the EXAFS spectra, (2) the absence of an intense pre-edge (1s → 3d) peak, from comparison with a Mn$^V$=N reference complex (Fig. 9) and (3) no Raman signal in the range of 900 → 1000 cm$^{-1}$ (Mn$^V$=O) was detected. The proposed structure for the green oxidized complex, based on these observations in the reactions with *m*-CPBA, is shown in Scheme 1.

Feth concluded that the product formed was a Mn$^{IV}$ intermediate complex, with an *m*-CPBA molecule is associated via a Mn–O single bond. A radical cationic structure of this complex (explaining its high reactivity) can be assumed from the observed absorption band at 640 nm. The product of the decay of the green
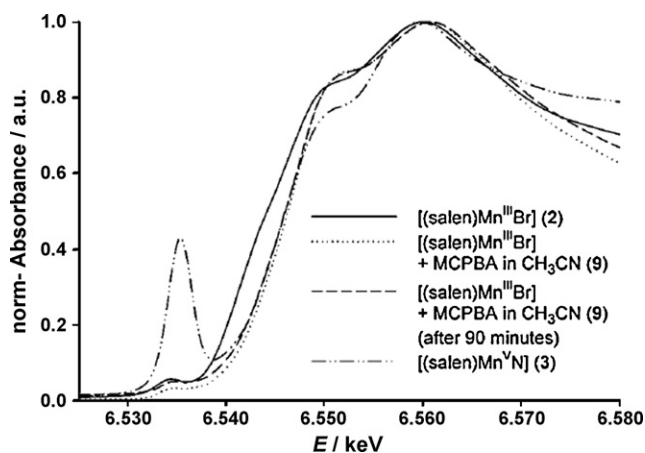
Fig. 9. Comparison of the Mn K-edge XANES regions of the oxidized [(salen)Mn$^{III}$Br], **12** in acetonitrile. Solid [(salen)Mn$^{III}$Br], **12**, oxidized with *m*-CPBA in acetonitrile after 0 min, oxidized with *m*-CPBA in acetonitrile after 90 min (dotted line), solid [(salen)Mn$^V$(N)], **13** (figure was reproduced from Ref. [66], Copyright (2003) Wiley–VCH Verlag GmbH & Co. KGaA).

Mn$^{IV}$ complex in CH$_2$Cl$_2$ could be a neutral Mn$^{IV}$=O species, as was proposed by Adam et al. [60], which would also explain the Raman signal at 725 cm$^{-1}$, observed in the solution during the oxidation with *m*-CPBA [66].

While much of the focus has been given to Mn$^V$=O complexes, Mn$^{IV}$=O or Mn$^{IV}$–OH complexes may also serve as useful models for the latter S-states of the water oxidation cycle. The work of Groves and coworkers on Mn porphyrin complexes has revealed a fair amount of information about the chemistry of the high valent states of complexes bearing these ligands [77]. The Mn$^V$-oxo porphyrins have been characterized with various spectroscopic techniques, including UV–vis, EPR, $^1$H and $^{19}$F NMR, resonance Raman, and X-ray absorption spectroscopy. These combined spectroscopic results indicate that the Mn$^V$-oxo porphyrins are diamagnetic low-spin (S = 0) species with a longer, weaker Mn–O bond (double bond) than in Mn$^V$-oxo complexes of non-porphyrin ligands [78]. However, if the oxidation reaction (of Mn$^{III}$-porphyrin) is conducted in the absence of base, (Porp)Mn$^{IV}$=O has been observed instead of the [(Porp)Mn$^V$=O]$^+$ species [78].

There is an important nomenclature point regarding the term "oxo" that deserves brief mention. An "oxo" group may be a fully deprotonated water molecule that serves as a bridge between two atoms, such as in a di-μ-oxo Mn$^{IV}$ dimer. Alternatively, a metal "oxo" that has significant p–π bonding to a

high-valent metal ion is referred to with the suffix -yl, such as in manganyl (Mn$^V$=O) and ferryl (Fe$^V$=O) complexes. The third possibility is a terminal oxo without significant π bonding.

Recently, Borovik and coworkers reported the synthesis of a non-porphyrin Mn$^{IV}$-oxo species of the latter variety, complex **14** was derived from the one-electron oxidation of the previously reported complex [Mn$^{III}$H$_3$buea(O)]$^{2-}$ [79]. The HBDE for the formation of this species has been reported to be rather large (~103 kcal/mol for Mn$^{III}$ → Mn$^{IV}$ and ≤80 kcal/mol for Mn$^{II}$ → Mn$^{III}$) [80] in contrast to previous values of ~80–90 kcal/mol reported by Busch and coworkers [37] for mononuclear Mn$^{IV}$ and Pecoraro and coworkers [81] for dimers. While the putative manganyl species, where the trapped oxygen atom is hydrogen-bonded by the amide of the functionalized urea ligand, has not yet been characterized by X-ray crystallography, the Mn$^{III}$ precursor provides a useful starting point, due to its structural characterization. The expected structural features of the "Mn–O" complex were derived from DFT calculations (Fig. 10). Thus, the Mn–O distance in the optimized structure is 1.706 Å, which is longer than can be expected for the comparable π bonded Mn$^V$-oxo complexes. From solution FTIR experiments in DMSO with $^{16}$O$_2$ as the oxidant they observed a new peak at 737 cm$^{-1}$, which shifted to 709 cm$^{-1}$ in the $^{18}$O-labeled sample. The authors claimed that their value is comparable to the ν(MnO) = 754 cm$^{-1}$ reported for [Mn$^{IV}$TMP(O)] [82]. It should be noted that the starting Mn$^{III}$-oxo complex and DMSO both have strong vibrations at ~700 cm$^{-1}$ that may overlap with the peak assigned as the Mn–$^{18}$O vibration. The frequencies of Mn–O–H bending modes in resonance Raman experiments are variable, but have been found in the ≈700 cm$^{-1}$ region for strongly H-bonded OH groups [83,84].

A very important distinction is to be made between Mn$^V$(O, as in Collins' compounds, which have electrophilic, formally δ$^+$ oxygens and the Borovik compound, **14**, which is at the other end of the spectrum. Although it has yet to be structurally characterized, one could expect such a compound to have more or less Mn–O single bonds and significant negative charge on the oxygen atom, which in this case is stabilized by H-bonding. Thus, this "oxo" is strongly basic and expected to behave as a nucleophile. Intermediate in behavior are the μ-oxo species, which are very weak bases as the coordinated metal atoms serve as pseudo-protons, lowering the oxygen basicity. Of specific importance to photosynthesis, manganyl species (Mn=O) activate an oxygen atom to be attacked by an electron-rich group, such as the Mn-"oxo" compound reported by Borovik. It is likely that the
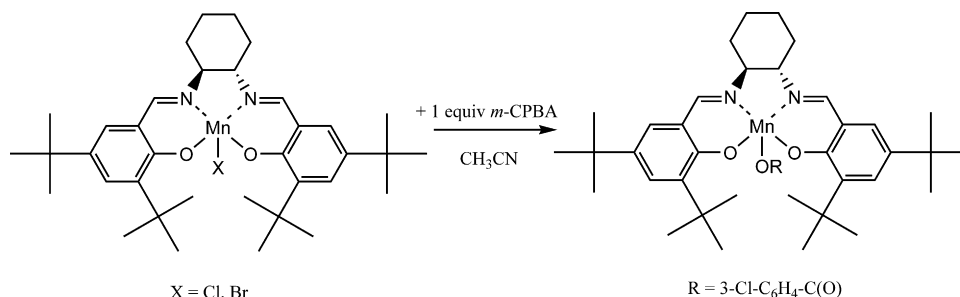


Scheme 1. Oxidation reaction proposed by Feth for Jacobsen olefin epoxidation catalyst (scheme was reproduced from Ref. [66], Copyright (2003) Wiley–VCH Verlag GmbH & Co. KGaA).
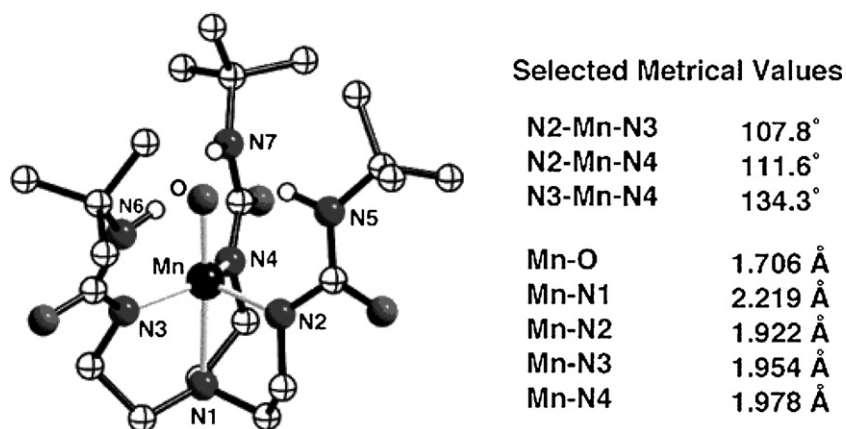
Selected Metrical Values

| | |
|---|---|
| N2-Mn-N3 | 107.8° |
| N2-Mn-N4 | 111.6° |
| N3-Mn-N4 | 134.3° |
| Mn-O | 1.706 Å |
| Mn-N1 | 2.219 Å |
| Mn-N2 | 1.922 Å |
| Mn-N3 | 1.954 Å |
| Mn-N4 | 1.978 Å |

Fig. 10. Molecular structure of $[Mn^{IV}H_3buea(O)]^-$, **14**, obtained from geometry-optimized DFT calculations (B3LYP/6-311G). Only urea hydrogen atoms are shown for clarity (figure was reproduced from Ref. [79], Copyright (2006) American Chemical Society).

differences in HBDEs reported by Pecoraro, Busch and Borovik are a result of these different oxo type structures. In particular, the strong basicity of the manganese oxide like "oxo" of Borovik is expected to markedly increase the HBDE (103 kcal/mol versus others at 80–94 kcal/mol). Manganyl, with significant oxygen π bonding will be more acidic and yield a different HBDE.

A group of novel complexes known as Hangman Porphyrins and Salophens have been reported recently by Nocera and coworkers [85,86–88]. Such ligands were specifically designed to position an acid-base functionality directly over a redox cofactor [86]. Manganyl functionalities have been implicated in a proposed mechanism for catalase-like activity. Positioning a proton donor above the metal ion, as in the Mn-HSX complexes, appears to the stabilize hydroperoxide adducts (as putative intermediates derived from DFT calculations) as is shown in Fig. 11 [86]. Although neither such complex has been structurally characterized by XRD, the authors have suggested the formation of a $Mn^V$-oxo species based on stopped-flow kinetic (UV–vis) experiments of HSX-$Mn^{III}$-SalophOMe, **15**, that were performed using *m*-CPBA as the O atom source [87]. The $Mn^V$ intermedi-



Fig. 11. Energy minimized structure (from DFT calculations) of the hydroperoxide complex of Mn-Saloph-OMe complex, **15**, reported by Nocera and coworkers (figure was reproduced from Ref. [86], Copyright (2005) American Chemical Society).

ate, $\lambda_{max} = 420$ nm, is proposed based on comparison with the analogous (and structurally characterized) $Mn^V$-nitrido which has a $\lambda_{max} = 459$ nm in the absorption spectrum. The $Mn^V$-oxo intermediate is transient, however, and only has a lifetime of several minutes, even at $-20\,°C$ [88]. At the moment, it appears that such intermediates warrant further investigation by time-resolved XAS and EPR experiments in order to provide a more direct comparison with the spectroscopic features observed in S-state progression of PSII. While these compounds have interesting reactivity that may ultimately prove catalytically fruitful, they bear little structural resemblance to the $Mn_4Ca$ catalyst found in the OEC.

### 3.2. Dinuclear Mn complexes

A multitude of dinuclear Mn complexes have been studied as possible models for the OEC. Many of these complexes have been reviewed thoroughly in recent years either by Armstrong [13] or in the recent review on the Mn Catalases by Wu et al. [14]. Additional reviews with a focus on inorganic aspects of photosynthesis examine the model compounds reported in the earlier literature [6,7,89]. As all the S-states are known to be primarily composed of $Mn^{III}$ or higher oxidation levels (the possible exception would be $S_0$, perhaps being $Mn^{II}Mn^{III}Mn_2^{IV}$) those complexes that consist of $Mn_2^{II}$ or $Mn^{II}Mn^{III}$ oxidation levels can be largely ignored when discussing the normal catalytic cycle of the OEC.

#### 3.2.1. Mn-μ-O-Mn

There are roughly 40 binuclear structures deposited in the Cambridge Structural Database (CSD) that have a single $\mu_2$-oxo bridge between to $Mn^{III}$ dimer centers. The vast majority (29 structures) of these also have two $\mu_2$-carboxylato bridges. Among the few (8) examples with a single $\mu_2$-oxo bridge is the 2005 report by Mascharak and coworkers with the structure of a dinuclear μ-oxo bridged $Mn^{III}$ complex, **16** (Fig. 12, left) derived from a polypyridine ligand with a single carboxamide group [90]. As shown later in this discussion, the physical properties associated with a mono-μ-oxo bridge may be useful for determining the viability of certain tetranuclear model
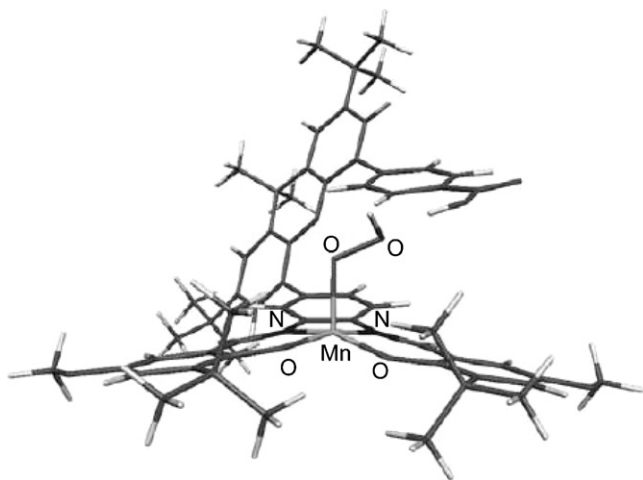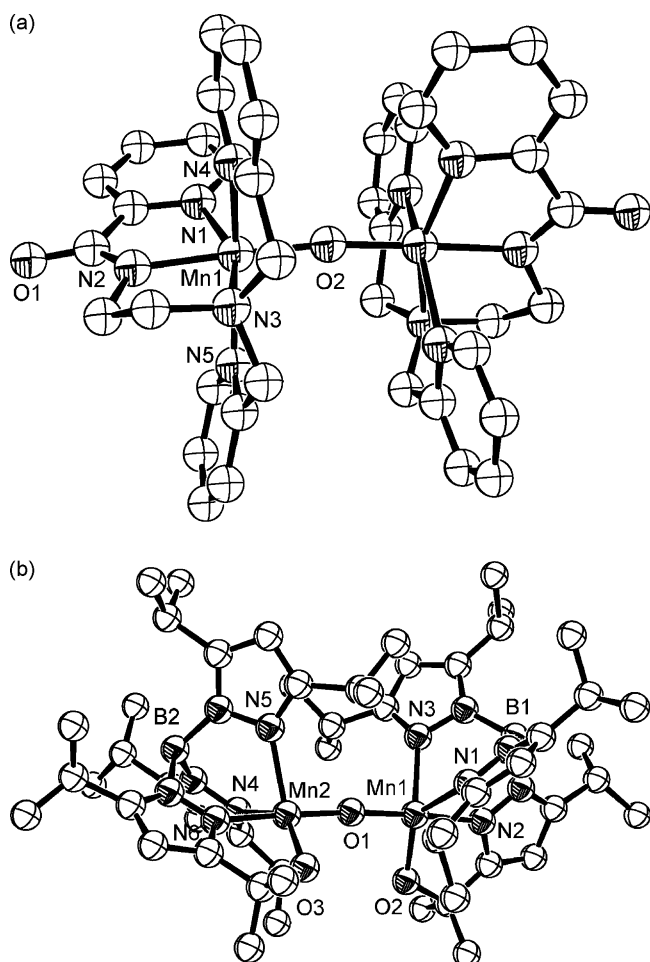
Fig. 12. ORTEP representations for dinuclear $Mn_2^{III}(O)$ complexes of (a) Mascharak, **16** (figure was reproduced from Ref. [90], Copyright (2005) American Chemical Society), and (b) the ligand hydroxylated complex reported by Kitajima, **17** (figure was reproduced from Ref. [93], Copyright (1991) American Chemical Society).

compounds [91,92]. The compound was synthesized from the analogous mononuclear $Mn^{II}$ complex by slow air oxidation, with the recrystallized product reported in 55% yield. A major drawback with regards to its suitability as an OEC model is the coordinative saturation of the Mn centers.

The single μ-oxo bridge in **16** is unstable toward proton donors. Protonation of the μ-oxo bridge destroys the dimer, allowing the corresponding anion to bind at the sixth site (trans to the carboxamido N). Examples of this reactivity have been noted with methanol, acetic acid, benzoic acid, and phenol. Optical spectroscopy has been employed to follow these reactions, for example, 2 equiv. of acetic or benzoic acid affords the green acetate complex ($\lambda_{max} = 570$ nm) or the green benzoate complex ($\lambda_{max} = 590$ nm). Interestingly, addition of NaOAc or NaOPh to a solution of **16** in acetonitrile does not result in a color change, suggesting that protons are required for the bridge-splitting reaction.

The oxidative ligand hydroxylation reaction of the $Mn_2^{II}$ dimer, $[Mn^{II}(HB(3,5-^iPr_2pz)_3)]_2(\mu\text{-OH})_2$, in the presence of $O_2$ was reported by Kitajima et al. [93]. A mechanism was proposed (Scheme 2a) that includes the formation of an interme-

diate with $\mu_2$-peroxo coordination followed by a $Mn^{IV}$ μ-oxo dimer intermediate with terminal oxo bonds to each Mn. This is a fascinating and important reaction as the first two steps, run in reverse, represent a process for oxidizing water by the Babcock mechanism (for which an adaptation by Sieg-bahn is shown in Scheme 2b) [94,95]. The end product is a ligand-(mono)hydroxylated complex $[Mn^{III}\{HB(3\text{-OCMe}_2\text{-}5\text{-Pr}^i pz)(3,5\text{-Pr}^i_2pz)_2\}]_2(\mu\text{-O})$, **17**, in which the coordination about each Mn center is $N_3O_2$ (Fig. 12, right). Thus, an open coordination site remains in this complex, although there is only a single example of further reactivity that has been demonstrated [96].

### 3.2.2. $Mn\text{-}\mu\text{-}O_2\text{-}Mn$

While a single μ-oxo bridge in the $Mn_2^{III}$ dinuclear complexes leads to long $Mn\cdots Mn$ distances and weak coupling, the incorporation of a second μ-oxo bridge dramatically decreases the metal-metal separation. Typical $Mn\cdots Mn$ distances within metal-oxo core are on the order of 2.67–2.70 Å with Mn–O–Mn angles between 92° and 97° [97]. The relationship between $Mn\cdots Mn$ distance and Mn–O–Mn angle has been quantified for such complexes. Chelating ligands with two or more nitrogen donors are often used to provide the terminal coordination sites for each Mn ion. The $Mn^{III}$ ions in these systems are strongly anti-ferromagnetically coupled ($J = -86.5$ to $-100.5$ cm$^{-1}$). While complexes with tetradentate ligands have $O_h$ geometry at the Mn centers, steric crowding of the monoanionic tridentate ligand, $HB(3,5-^iPr_2pz)_3^-$, restricts this complex, **18** (Fig. 13) to a penta-coordinate geometry about each Mn ion [98]. The solution electronic spectra of these complexes are characteristic of the $[Mn_2(\mu\text{-O})_2]^{2+}$ core with two rather intense bands in the region between 400 and 600 nm [6].

Di-$\mu_2$-oxo $Mn_2$ complexes have been among the most intensively studied, and most important models, for the OEC. The reason for the importance of these molecules is quite varied. In the mixed valence form, they provided spectral evidence that the OEC contained a cluster of manganese in different oxidation states. They showed the first 2.7 Å Mn–Mn separations [99],



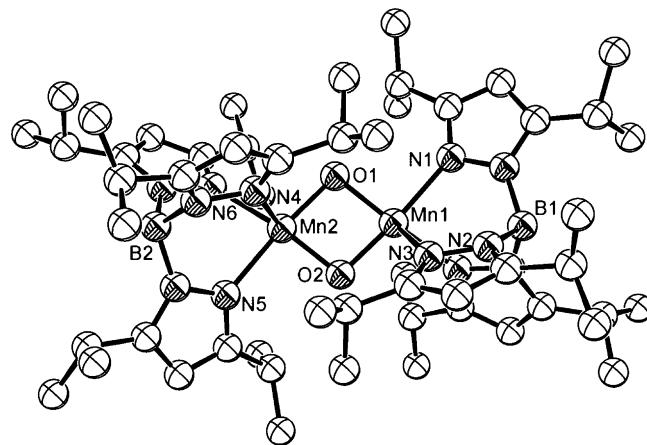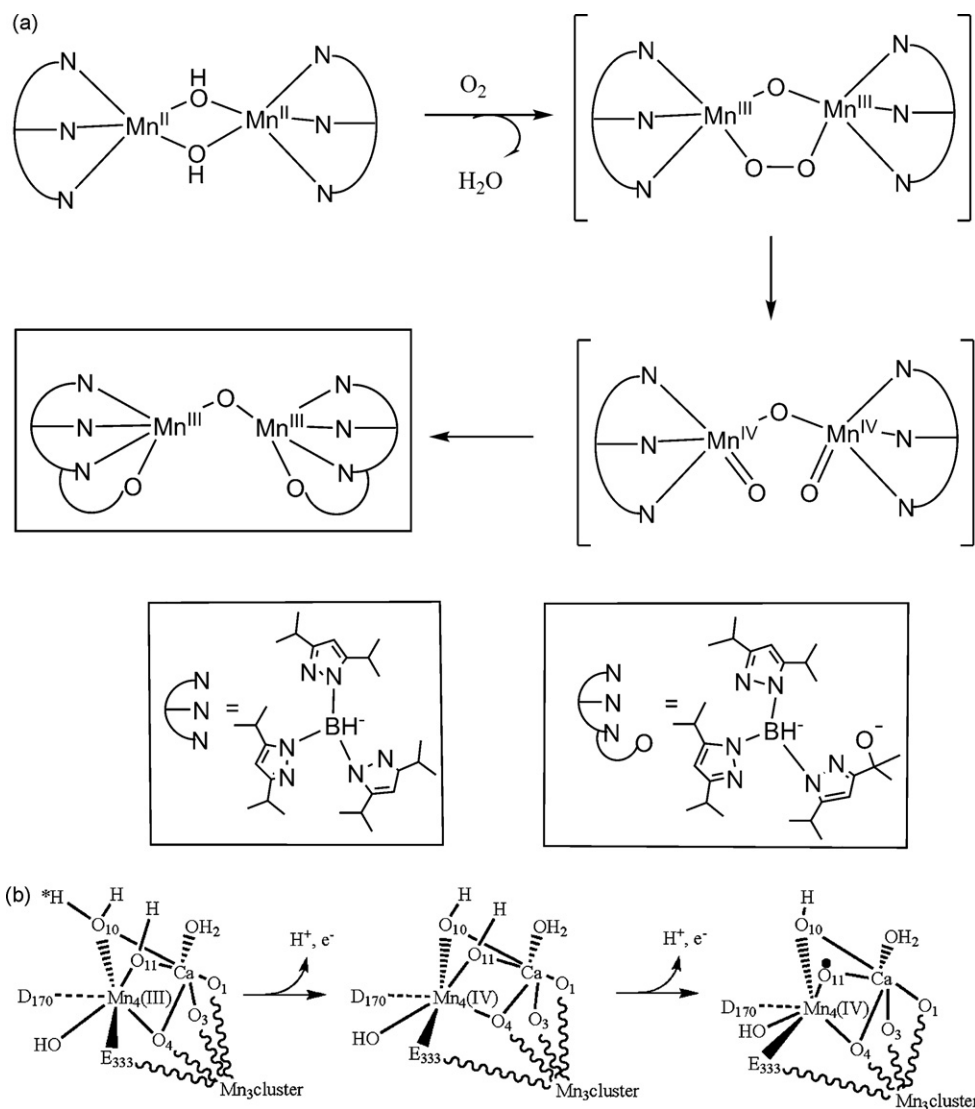Fig. 13. ORTEP representations for dinuclear complex, $[(HB(3,5-^iPr_2pz)_3)Mn^{III}(\mu\text{-O})]_2$, **18**, reported by Kitajima and coworkers (figure was reproduced from Ref. [98], Copyright (1991) American Chemical Society).

Scheme 2. (a) Mechanism proposed by Kitajima for the oxidative ligand hydroxylation via a bis(Mn$^{IV}$=O) intermediate (figure was reproduced from Ref. [93], Copyright (1991) American Chemical Society) and (b) mechanism proposed by Siegbahn based on DFT calculations for the latter S-state transitions in the OEC (figure was reproduced from Ref. [95], Copyright (2004) PCCP Owner Societies).

the distance that forms the structural hallmark of the catalytic center and served as the basis for testing the famous "Dimer of dimers" structural model for the enzyme [99–101]. In addition, studies of the reactivity to form and destroy the dimers, along with perturbations of the properties upon protonation of these oxo bridges has proved critical to the viability of more recent water oxidation proposals [102–104].

In the late 1970s and early 1980s mixed valent (Mn$^{III}$Mn$^{IV}$) complexes using bipyridyl ligands were synthesized, structurally characterized [105] and spectroscopically interrogated [21,106–108]. Dismukes recognized the similarity between the multiline signal observed in the EPR spectrum for these dimers ($g = 2$, 16 lines) and that of the OEC in the S$_2$ ($g = 2$, 19–22 lines) [109–111]. Based on the magnitude of the hyperfine coupling constants and energy of the transition, it was concluded that the OEC contained a mixed valence manganese cluster [112]. Subsequent analysis suggested that to simulate the OEC spectrum, one needed a cluster of at least three and then four manganese

ions to match the EPR, ESEEM and ENDOR spectra [113–115]. Thus, this and related Mn$^{III}$Mn$^{IV}$ species played a crucial role in our early understanding of the enzyme.

Compared to the relatively small number of bis($\mu$-oxo) Mn$_2$$^{III}$ complexes, there are a numerous examples of the corresponding Mn$^{III}$Mn$^{IV}$ cores [13]. At temperatures below 77 K in frozen solutions, all known Mn$^{III}$Mn$^{IV}$ bis($\mu$-oxo) complexes display the typical 16–19-line EPR signal centered at $g \approx 2$ (similar to the spectra shown in Fig. 14) [116]. As discussed later in this current review, complexes of this mixed-valence state have served as some of the best functional models for water oxidation to date [92,117].

Another important property of Mn$^{III}$Mn$^{IV}$O$_2$ and Mn$_2$$^{IV}$O$_2$ species is the observed Mn–Mn separations which typically are $2.7 \pm 0.1$ Å [119–121]. Tri $\mu_2$-oxo compounds have much shorter distances ($\sim$2.30 Å) [122], di-$\mu$-oxo, monocarboxylato [123] or di-$\mu$-oxo, peroxo [124,125] species have distances of 2.54–2.6 Å and mono-$\mu$-oxo, dicarboxylato structures, such
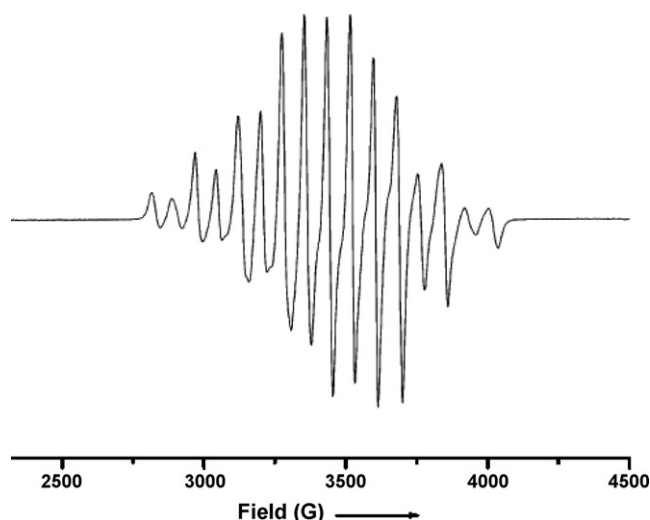
Fig. 14. Typical X-band 16-line EPR signal [13,116,118] for a dinuclear Mn[III]Mn[IV] complex (figure was reproduced from Ref. [13], Copyright (2004) American Chemical Society).

as found in Mn catalases are around 3.3 Å [126,127]. These ranges set limits upon the reasonable structure types for the enzyme when only EXAFS data were available. In particular, the observed 2.7 Å distance was assigned as Mn–Mn interactions, whereas the longer Mn–M distance of 3.3 Å was assigned as either Mn–Mn or Mn–Ca [128–132].

After the bipyridyl Mn dimers, $[Mn_2^{IV}(\mu_2\text{-O})_2(SALPN)]_2$, **19**, is probably the next most important structure of this class. Boucher and coworkers [102,133] first reported the synthesis of this complex although Pecoraro and coworkers [99,134] and Armstrong and coworkers [135] independently first reported the structure. One of the most important early reactivity studies suggested that the addition of $H^+$ to **19** claimed that the Mn[III] monomer was formed with the liberation of hydrogen peroxide [133]. This observation was very exciting, especially given two other results. In the early 1990s, Larson and Pecoraro demonstrated that the reaction of hydrogen peroxide with **19** gave a very efficient catalase reaction ($2H_2O_2 \rightarrow O_2 + 2H_2O$) [134]. Secondly, around the same time, the dimer of dimers model for the OEC was suggested. Thus, a very appealing model for water oxidation resulted. A dimer of dimers structure might exist with one dimer responsible for generating an O–O bond at the oxidation level of peroxide and the second dimer would be responsible for oxidizing this species to liberate dioxygen [101,136]. Such a model gained further support from the observation of Tolman that $Cu_2(\mu_2\text{-O})_2$ species could reversibly convert between $Cu^{III}(\mu_2\text{-O})_2$ and $Cu^{II}(O_2)$ structures [137]. Unfortunately, the enthusiasm for this model was quenched when it was realized that the Boucher and Coe claim for peroxide formation was incorrect, and that SALPN oxidation occurred rather than liberation of peroxide [138]. Subsequently, X-ray studies now suggest that the best description for the OEC is an $Mn_4Ca$ structure with the fourth manganese acting as a dangler [16–18].

Despite this setback, the chemistry of $[Mn_2^{IV}(\mu_2\text{-O})_2(SALPN)]_2$ ultimately provided numerous important results for water oxidation chemistry [10]. First, an analysis of this and

other anti-ferromagnetically coupled Mn dimers suggested that the dimer of dimers model was inconsistent with the magnetic [139] and spectroscopic [140] properties of the OEC. Important to this analysis was the recognition that in $S_2$, two different EPR signals could be observed with no apparent structural perturbations (as assessed by EXAFS spectroscopy) [131]. The first signal, the $g = 2$ multiline came from an $S = 1/2$ ground state. The second signal, a broad, low field feature that was centered at $g = 4.1$, had an $S = 5/2$ ground state [141]; although Brudvig and coworkers made an argument for $S = 3/2$ to describe this feature [142]. Given the known oxidation states for $S_2$ ($Mn^{III}Mn_3^{IV}$), there was no way that one could rationalize these two signals within a dimer of dimers topology. This led Pecoraro and coworkers [10] to suggest a $3 + 1$ cluster formulation as is shown in Fig. 15A. Looking at the Mn topology alone, this proposed structure bears striking resemblance to the present view (Fig. 15B and C) of the cluster after adding calcium which one
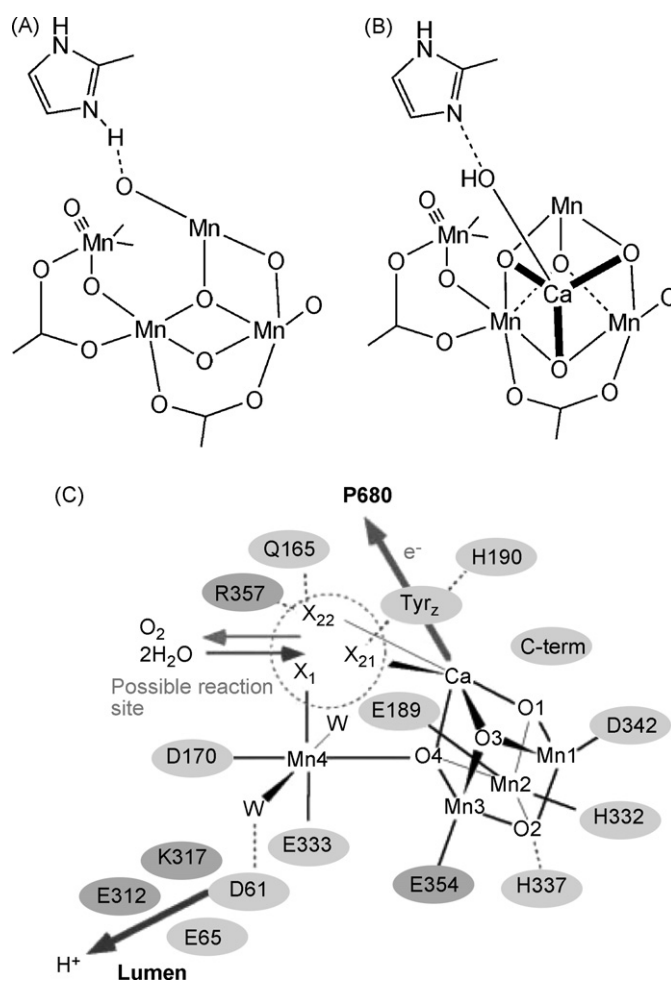


Fig. 15. (A) structural proposal [10] of the OEC based on a simple magnetic analysis prior to the Zouni X-ray structure. (B) Diagrammatic representation of the OEC based on more recent X-ray structures. Notice that the Mn connectivity appears to match well with respect to the simple magnetic model in part A, differing by one Mn–O–Mn connection and the addition of a $\mu_2$-O bridge. Ca(II), whose presence could not be inferred from the magnetic analysis because it is diamagnetic, nicely caps the structure. (C) OEC structure proposed by Barber for comparison (figure was reproduced from Ref. [16], with permission from AAAS).

could not locate via a magnetic analysis because it is diamagnetic. Subsequent EPR spectral analysis predicted the dangler model, which also is close to the presently accepted metal topology [139].

However, **19** has also been an important molecule defining the formation of μ-oxo bridged Mn clusters and the properties of these structures upon protonation. As an example, the first detailed studies determining the p$K_a$ for such Mn$^{IV}$ structures were determined and it was shown that protonation of the oxo bridges led to a perturbation of the redox potential and a significant decrease in the anti-ferromagnetic coupling of the system [103]. In particular, it was studies such as these that demonstrated that protons were as important as electrons for the reactivity of these systems. As an example, protonation or methylation of the oxo-bridge destroyed the catalase activity of these compounds. Possibly most important, these were the first manganese oxo bridged molecules for which homolytic bond dissociation energies were reported [104]. These data demonstrated that the energetics of water oxidation were precisely tuned to both the proton and the electron and that proton coupled electron transfer (PCET) or H-atom abstraction were likely to be involved in water oxidation chemistry [9,89,143].

While generally of lesser importance to the understanding of photosynthetic water oxidation, alkoxo bridge dimers have made some significant contributions to the field. Probably foremost among these complexes are dinuclear complexes formed using the ligand 2-OH-SALPN [104,144,145]. This ligand differs from SALPN by the addition of a hydroxyl group to the propylenediamine backbone. This apparently minor modification leads to markedly different chemistry [145]. Whereas dimers of the type [Mn$^{IV}$(μ$_2$-O)(SALPN)]$_2$ are the dominant isolated structure with SALPN, 2-OH-SALPN leads to dinuclear structures with alkoxy bridges such as [Mn$^{II}$(2-OH-SALPN)]$_2^{2-}$. In fact, four distinct oxidation levels of this structure have been isolated [Mn(2-OH-SALPN)]$_2^{2-\ to\ 1+}$ [146]. The Mn–Mn separations remain within 0.1 Å across this series (~3.2–3.3 Å) and the reduction potential for each successive compound shifts by ~350 mV. A related series of compounds have also been prepared {[Mn$^{III}$(2-OH-SALPN)]$_2$(L)} which contain a terminal ligand such as water or alcohol [81,115,146,147]. These later compounds were particularly important for establishing the HBDEs for coordinated water protons. An HBDE ~87 kcal/mol was observed (range of 84–92 kcal/mol), slightly higher than for deprotonation of μ$_2$-OH units, going from the Mn$_2^{III}$(OH$_2$) to Mn$^{III}$Mn$^{IV}$(OH) and Mn$^{III}$Mn$^{IV}$(OH$_2$) to Mn$_2^{IV}$(OH) species. These studies were especially important when assessing the thermodynamic viability of the Babcock water oxidation proposal since a tyrosyl radical in a protein is thought to provide the same energy for H atom abstraction [81].

A second important contribution made through the study of this system was a better understanding of Mn oxidation reactions with hydrogen peroxide and alkyl peroxides. The [Mn$^{II}$(2-OH-SALPN)]$_2^{2-}$ is one of the best reactivity mimics of the manganese catalases [145,146]. More important for photosynthetic chemistry, detailed studies of [Mn(2-OH-SALPN)]$_2$ with alkyl peroxides have been performed. While this reaction leads to vigorous liberation of dioxygen in the presence of
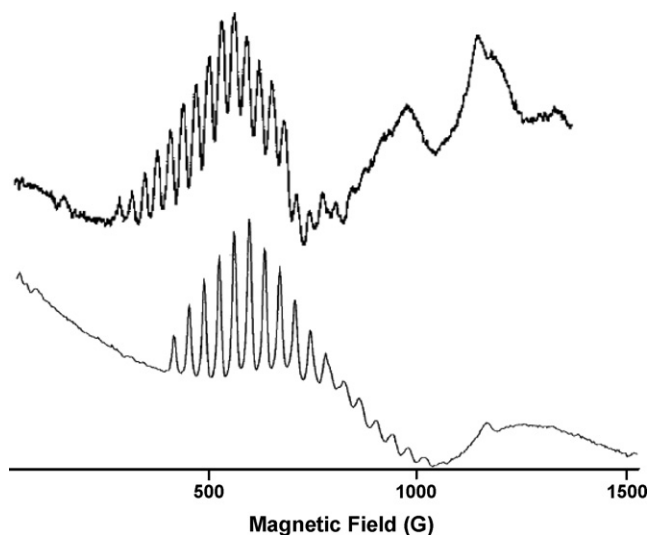


Fig. 16. Comparison of the parallel-mode EPR spectra of the S$_1$ state in OEC [148] (top) and the spectrum associated with a proposed {[Mn$^{IV}$(2-OH-SALPN)]$_2$(μ$_2$-O)[Mn$^{IV}$(2-OH-SALPN)]$_2$}$^{2+}$ complex, **20** (bottom) (figure was reproduced from Ref. [147], with permission of copyright holders Elsevier (2004)).

excess *t*-butyl peroxide, this does not represent a water oxidation process. Instead, *t*-butyl peroxide radicals are generated which chain propagate, ultimately forming the (*t*-butyl)OOOO(*t*-butyl) species which liberates singlet dioxygen and regenerates *t*-butylOO$^\bullet$. Thus, any reaction claiming oxygen evolution using *t*-butyl peroxide must make every effort to ensure that this alternative radical process is not occurring [104].

The final significant contribution that has come from the studies of Mn(2-OH-SALPN) system was the formation of a tetrameric complex thought to be {[Mn$^{IV}$(2-OH-SALPN)]$_2$(μ$_2$-O)[Mn$^{IV}$(2-OH-SALPN)]$_2$}$^{2+}$, **20**. This species exhibits a complicated multiline feature at low field in the parallel mode EPR spectrum. In fact, as shown in Fig. 16, it exhibits a striking resemblance to the parallel mode signal observed for the OEC in S$_1$ [147]. There is a slight shift in g value and the hyperfine coupling constants are slightly smaller in the 2-OH-SALPN model complex. This is as expected since the model is two oxidizing equivalents higher than that of S$_1$. Nonetheless, there are no other small molecule models that have been reported that show such a low field multiline signature in the parallel mode spectrum. Hence, based on EPR spectroscopy, this is the best known model for S$_1$.

### 3.2.3. *Mn-μ-O$_2$-μ-(O$_2$)-Mn*

In 1990, Wieghardt and coworkers reported the preparation of the dinuclear Mn$^{IV}$ complex [Mn$_2^{IV}$L$_2$(μ-O)$_2$(μ-O$_2$)]$^{2+}$, **21**, via the *in situ* aerobic oxidation of a Mn$^{II}$-Me$_3$TACN precursor [124]. The X-ray crystal structure of this complex (Fig. 17) revealed that the Mn ions are linked by one peroxo and two oxo bridges with the 1,4,7-trimethyl-1,4,7-triazacyclononane ligand occupying the terminal coordination sites. The complex was found to be relatively stable (many hours) in acetonitrile solution while decomposing rapidly in aqueous solution under anaerobic conditions (Ar) at 20 °C, with the release of dioxygen as was
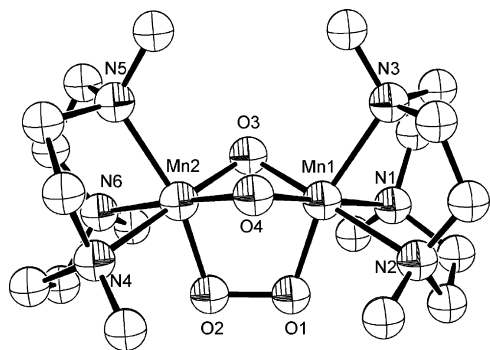
Fig. 17. Molecular structure of $[Mn_2^{IV}L_2(\mu\text{-}O)_2(\mu\text{-}O_2)]^{2+}$, **21** (L = 1,4,7-trimethyl-1,4,7-triazacyclononane) derived from X-ray crystallography (figure was reproduced from Ref. [124], Copyright (1990) American Chemical Society).

established by GC analysis, mass spectrometry, and measurements with an oxygen electrode. The reduction of $Mn^{IV}$ yielded a binuclear $Mn^{III}$ intermediate which further degraded to form a stable $[LMn^{IV}(\mu\text{-}O)_3Mn^{IV}L]^{2+}$ species and a $Mn^{II}$ dimer, which is thought to dissociate to a mononuclear species $LMn(OH_2)_3]^{2+}$ and then rapidly be oxidized back to a $Mn^{III}$ species. This complex also suggests a manner similar to the Kitajima complexes discussed earlier, to form peroxide from terminal oxo's on high valent Mn ions.

### 3.2.4. Imidazolate bridged Mn dimers

In the 1990s it was proposed from EPR and ENDOR studies that a histidine bound to the manganese cluster could be consistent with an imidazolate bridge between two Mn centers [112]. Earlier studies had suggested a bridging motif for $NH_2^-$ in ammonia-treated $S_2$ samples [40,149]. To address the issue of imidazolate bridging in high oxidation states of the OEC, Pecoraro and coworkers first reported the structure of $[Mn_2^{IV}(dtbsalpn)_2(DCBI)]PF_6$, **22**, shown in Fig. 18(left) [150]. This complex exhibited unprecedented low temperature EPR signals due to a very weak anti-ferromagnetic coupling between the two $Mn^{IV}$ ions. In a subsequent paper, the synthesis and physical properties of the one- and two-electron reduced $Mn^{III,IV}$, **23** (Fig. 18, right) and $Mn^{III}_2$ forms were reported [151]. The mixed valent compound was shown to be the first example of a ferromagnetically coupled $Mn^{III}Mn^{IV}$ dimer. From the EPR data, it was shown that the mixed-valence $Mn^{III,IV}$ complex can be weakly ferromagnetically exchange coupled to exhibit an excited state $g = 2$ multiline signal.

### 3.2.5. Proposed catalytic dinuclear Mn models

The $Mn^{III,IV}$ terpyridine complex, **24** (Fig. 19a) was reported by Brudvig and coworkers to serve as the first model for catalytic O–O bond formation that employed typical oxidants such as sodium hypochlorite or $KHSO_5$ [152]. It has since been suggested that the dioxygen released comes about via a disproportionation reaction [153]. Collomb and coworkers explored this system via electrochemical methods [154,155]. These authors independently synthesized and reported the crystal structure of complex **24** at the same time as Brudvig and coworkers [156]. From these electrochemical studies in aqueous solution; oxidation of this
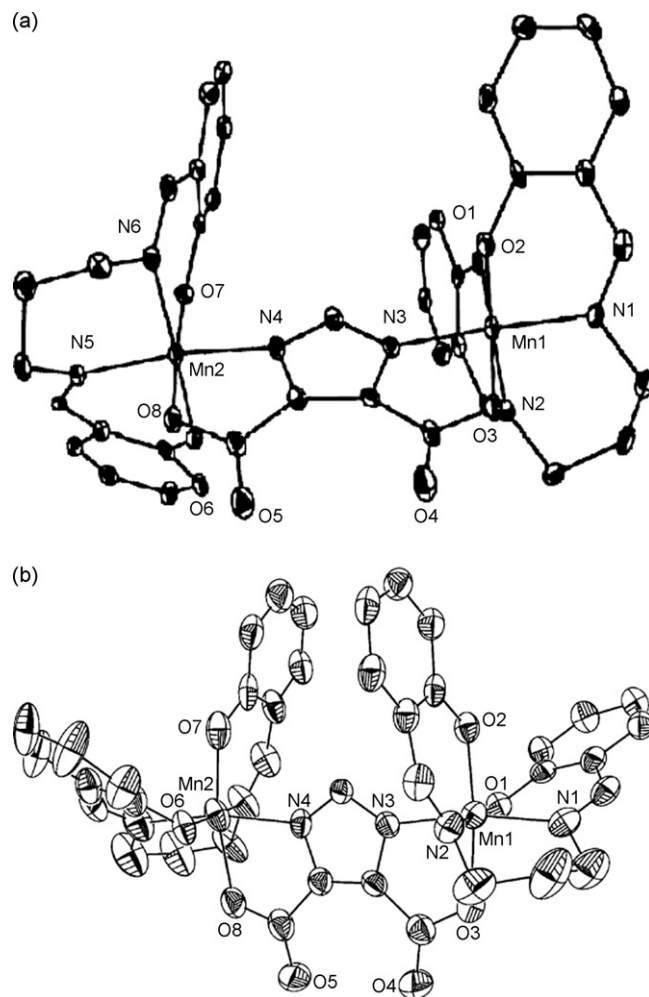


Fig. 18. ORTEP representations of (a) $[Mn^{IV}(dtbsalpn)]_2DCBI^+$ cation, **22** (figure was reproduced from Ref. [150], Copyright (1997) American Chemical Society) and (b) $[Mn^{III/IV}(dtbsalpn)]_2(DCBI)$, **23** (figure was reproduced from Ref. [151], by permission of The Royal Society of Chemistry); the *t*-butyl groups were removed from the 3,5-positions of the aromatic rings for clarity in both cases.

compound quantitatively yields the stable tetranuclear $Mn^{IV}$ complex, $[Mn_4^{IV}O_5(terpy)_4(H_2O)_2]^{4+}$ having a linear mono-$\mu$-oxo$\{Mn_2(\mu\text{-}oxo)_2\}_2$ core (compound **43** on page 48) [153]. Therefore, these results show that the electrochemical oxidation of $[Mn_2O_2(terpy)_2(H_2O)_2]^{3+}$ is only a one-electron process leading to **43** via the formation of a mono-$\mu$-oxo bridge between two oxidized $[Mn_2^{III,IV}O_2(terpy)_2(H_2O)_2]^{3+}$. **43** is stable in aqueous solution and thus unable to oxidize water. However, only the $Mn^{IV}$ oxidation state can be reached by electrochemical oxidation in water and $\mu$-oxo bridges are formed rather than terminal oxo ligands. In a related study, it was found that when trifluoroacetate is used as the supporting electrolyte, the instability of the one-electron oxidized species, $[Mn^{IV}(terpy)(N_3)_3]^+$, results in a reaction with residual water to form the di-$\mu$-oxo dimanganese(III,IV) complex, with the release of two protons and three azide anions [155]. Whereas the $Mn^{III}Mn^{IV}$ and $Mn_2^{IV}$ di-$\mu$-oxo complexes (with trifluoroacetate co-ligands) are stable, the reduced $Mn_2^{III}$ derivative was shown to reversibly disproportionate to mononuclear $Mn^{II}$ and $Mn^{IV}$ [154]. Most importantly,
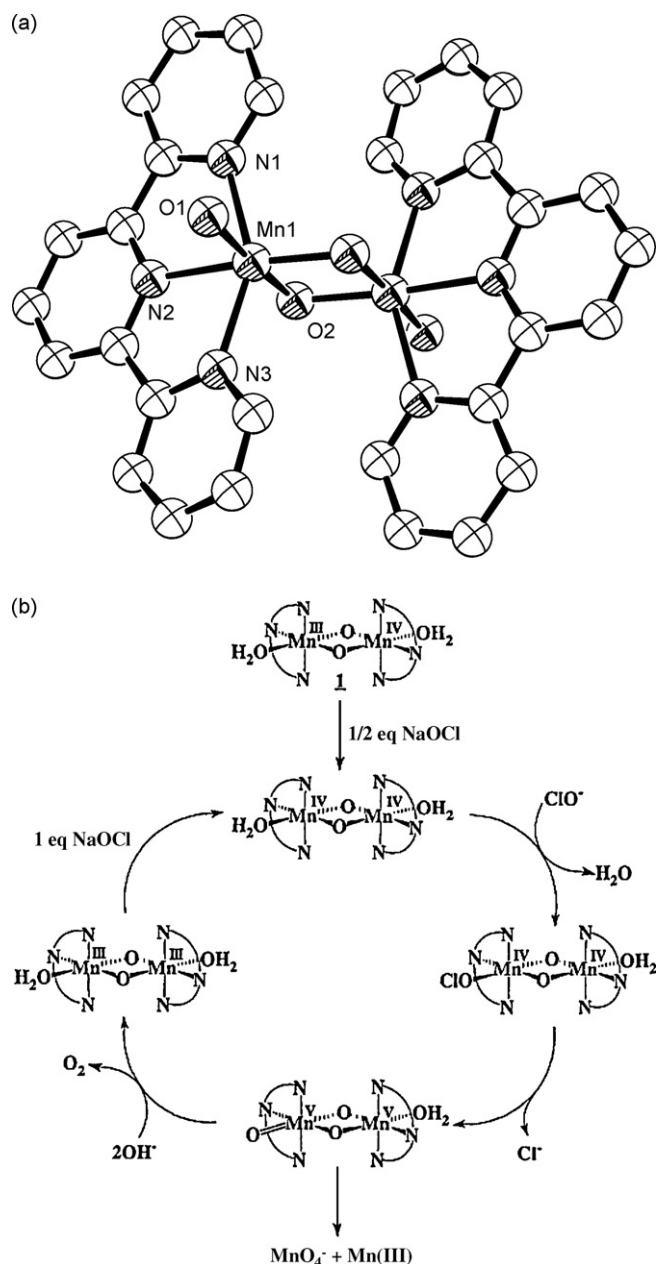
(a)



(b)



Fig. 19. (a) Dinuclear Mn catalyst, **24** and (b) the mechanism proposed by Brudvig and coworkers for O$_2$ production (figures reproduced from Refs. [152,158], with permission from AAAS).

the Mn$^V$≡O intermediate proposed in the earlier reports by Brudvig (Fig. 19b) was not observed in the present study; only the Mn$_2^{IV}$ oxidation state can be reached by electrochemical oxidation in acetonitrile. The presence of the trifluoroacetate ligands may prevent the formation of a possible Mn$^V$≡O species. Despite these solution studies, Yagi has shown that these water oxidation catalysts are effective when placed on a clay surface [157].

More recently (2005) McKenzie and coworkers have used a similar complex to probe reactivity towards the mechanistic model highlighted in Scheme 3, using *t*-butyl hydroperoxide as an oxidant [117]. It is well known that singlet dioxygen can be liberated from the reaction of Mn dimers and *t*-butyl hydroxide

[104]; however, it appears that this could be a genuine water oxidation process as $^{18}$O-labeled water is found in the dioxygen product. A highly reactive Mn$_2^{IV}$ species was suggested to play a crucial role in this process. Mechanistically this process resembles the oxo to peroxo route proposed by Boucher and coworkers [102,133], Tolman (for copper chemistry) [137], Yachandra et al. [159] and Dismukes and coworkers [160]. Further definition of this system is needed, with particular attention being focused on the origin of the second oxygen atom.

Naruta and coworkers have reported a water oxidation cycle (possibly catalytic) that has been proposed to include a dinuclear Mn$^V$-oxo porphyrin intermediate, **25** [161]. A representation of this process is displayed in Scheme 4. While there are several examples of well-characterized oxomanganese(V) porphyrin complexes that are capable of performing organic oxidations [162–164] this is among the first to incorporate two linked Mn-porphyrin moieties. The proposed cycle, which uses *m*-CPBA as an external oxidant, is shown in Scheme 4.

Already, much work has begun to design functional catalytic systems aimed at mimicking the light-induced single-electron transfer and charge-separating functions found in PSII. Styring and coworkers have studied mixed Ru–Mn complexes with such goals in mind [165]. To study the photophysical properties of Mn-containing OEC model systems these authors have reported several molecular iterations that are aimed at the eventual design of a charge-separating "functional" model [166,167]. However, studies performed with the dimeric Mn model depicted in Fig. 20 are worthy of discussion here. The RuMn$_2$ complex, **26**, may be oxidized from the Mn$_2^{II}$ to the mixed-valent Mn$^{III}$Mn$^{IV}$ state only when water is present. The authors have suggested that water serves to displace acetate as a ligand and eventually leads to water-based (oxo) ligands in the oxidized state. Such a reaction process seems to support mechanistic proposals that involve oxo-bridge formation (from coordinating water) during the S-state cycle. Related studies by Collomb and coworkers have been aimed at coupling Mn complexes having (μ-O)$_2$ bridges to photoactive Ru(bipy) units, to study the electron transfer chemistry [168,169] (Fig. 20).

### 3.3. Trinuclear Mn complexes

During the late 1980s there was discussion of an OEC catalytic center that had a mononuclear Mn center in close proximity to a trinuclear center [5]. Consideration of such a model was abruptly ended when Klein and coworkers demonstrated a multiline component with a $g \approx 4.1$ signal of the S$_2$ state after treatment of samples with ammonia [40]. However, beginning in 2000, suggestions of a 3 + 1 structural model emerged based on magnetic, spectroscopic, and crystallographic studies. Thus, the importance of studying the properties of trinuclear clusters has re-emerged.

#### 3.3.1. Basic carboxylate

Trinuclear Mn clusters may utilize a variety of possible structure types. The most simplistic arrangement is the Mn$_3$O core, in which all three metal ions are linked by oxygen and further ligated by carboxylates. This core type is frequently referred to
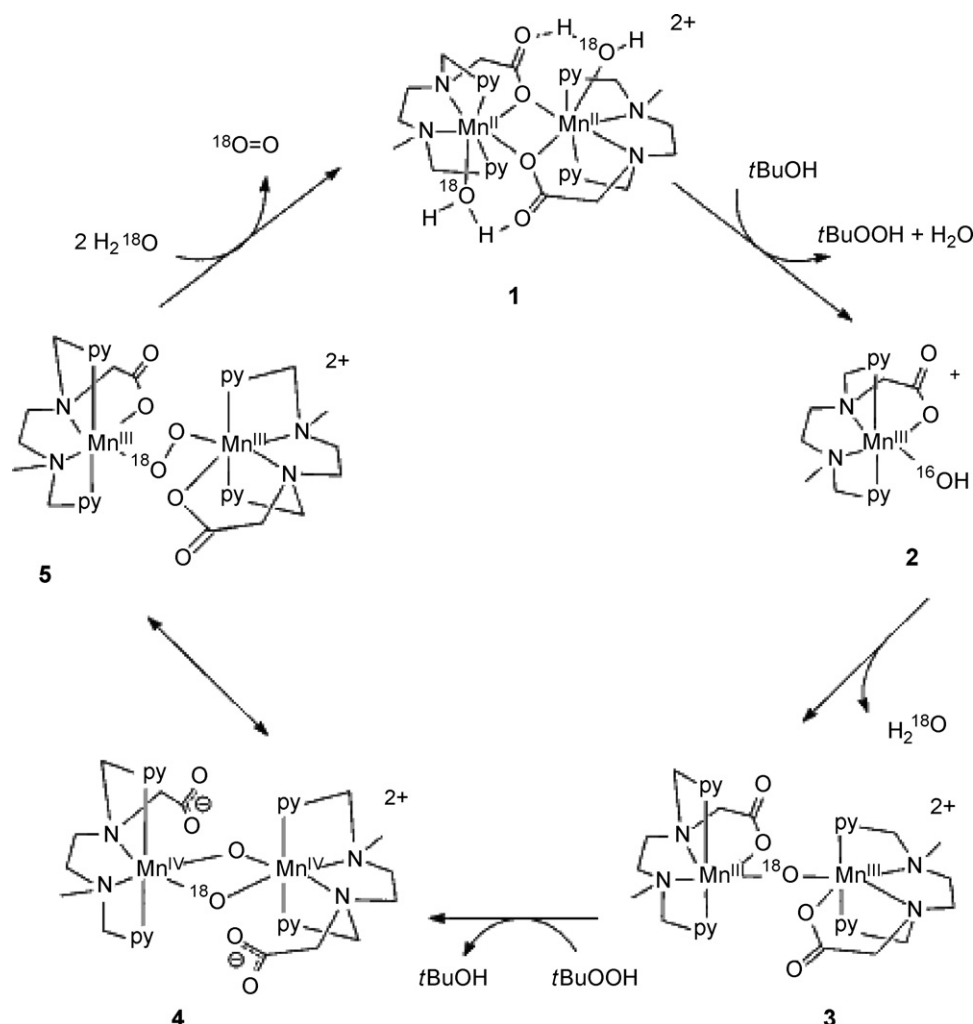
Scheme 3. McKenzie's proposed mechanism for water oxidation catalyzed by a dinuclear Mn complex using *t*-BuOOH as the O-atom source (scheme was reproduced from Ref. [117], Copyright (2005) Wiley–VCH Verlag GmbH & Co. KGaA).

as the basic carboxylate type [170]. As a noteworthy variant of this motif, Weatherburn and coworkers reported complex **27**, in which an oxo, peroxo and two carboxylato bridges link the Mn centers, with the peripheral sites occupied by three nitrogenous donors (from diethylenetriamine) per Mn (Fig. 21) [171]. This complex was the first instance reported with dioxygen coordinated to a trinuclear manganese cluster, though the quality of the crystal structure was less than ideal. Unlike the peroxo bridged dimer of Wieghardt and coworkers [124], the formal $Mn^{III}$ oxidation state of each metal center most likely excludes this compound as a higher S-state model as it is too low in oxidation state to be of relevance to $S_3$ or $S_4$. Nevertheless, one can envision this compound as modeling a di-$Mn^{IV}$=O that collapses to a 1,2-bridged $Mn^{III}$ peroxo species.

### 3.3.2. Linear versus bent structures

The open or linear structure type is another interesting structural class; where the early mixed valent $Mn^{III}Mn^{II}Mn^{III}$ clusters are of special interest. Despite the fact that they are far too low in oxidation state to be directly relevant to OEC chemistry, they have been used to address a few issues in photosynthesis. Pec-

oraro and coworkers reported the first such case, a tridentate Schiff base complex, **28**, with bridging acetate and terminal methanol ligands completing the coordination sphere (Fig. 22) [172,173]. Although a neutral complex, the oxidation state of the terminal manganese ions could not be assigned solely from the crystallographic data. To resolve the protonation-state ambiguity of the coordinated solvent, the isostructural THF analogue was prepared. This complex possessed identical magnetic and spectroscopic properties. As THF has no dissociable protons, the THF moiety must be coordinated as a neutral ligand in this neutral complex, thus the oxidation state of the terminal manganese atoms were established as +3 ions [172]. All of the trinuclear species in this class are valence trapped, with the $Mn^{III}$ ions showing marked Jahn–Teller distortions.

Bent trinuclear structures are also very important to understanding the spectroscopic features of the OEC, as they may provide useful comparisons of their physical properties to those typically found with a linear framework. Asato and coworkers used a macrocyclic Schiff-base complex obtained by the reaction of 2,6-diformyl-4-methylphenol with 1,11-diamino-3,9-dimethyl-3,9-diazo-6-oxaundecane to
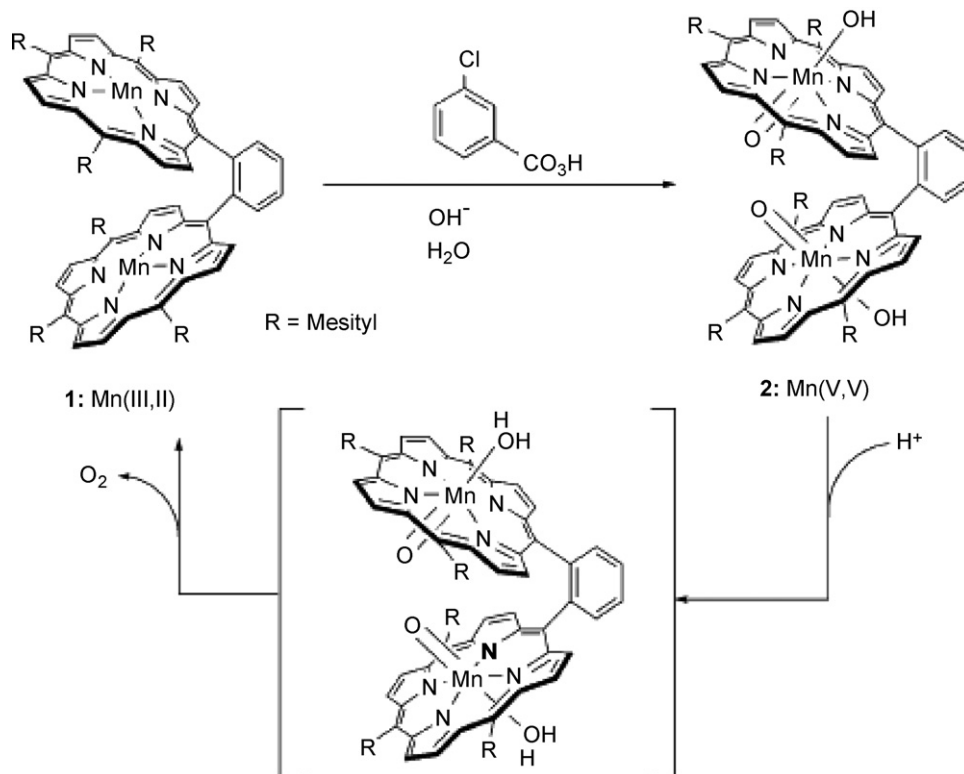
Scheme 4. Structure for the dinuclear structure [Mn(DTMP)]$^{2+}$, **25**, and the reaction pathway proposed by Naruta and coworkers for O$_2$ formation (scheme was reproduced from Ref. [161], Copyright (2004) Wiley–VCH Verlag GmbH & Co. KGaA).
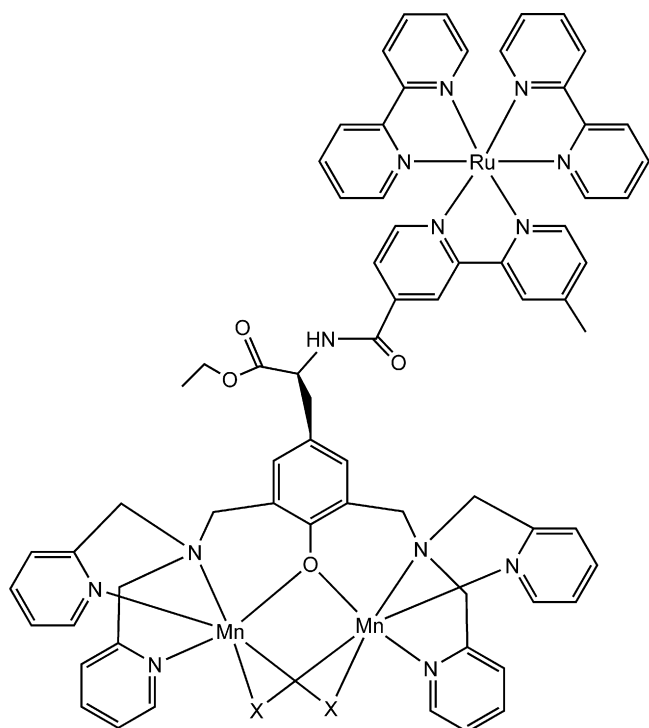


Fig. 20. RuMn$_2$ model complex, **26**, designed to explore multiple light-induced electron transfer reactions. The Mn oxidation states may be II$_2$ (with X = acetate), II,III (with X = acetate and H$_2$O/OH$^-$), III$_2$ (X = H$_2$O/OH$^-$), and III,IV (X = O$^{2-}$) (figure was reproduced from Ref. [165], Copyright (2006) Springer).
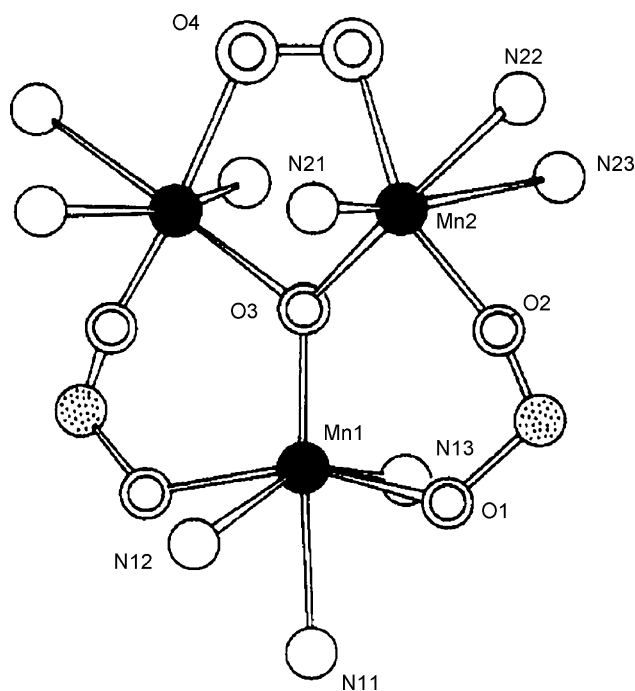


Fig. 21. Molecular structure of Mn$_3$$^{III}$(dien)$_3$($\mu$-OAc)$_2$($\mu_3$-O)($\mu$-O$_2$)$^{3+}$, **27**, derived from X-ray crystallography (figure was reproduced from Ref. [171], Copyright (1988) American Chemical Society).
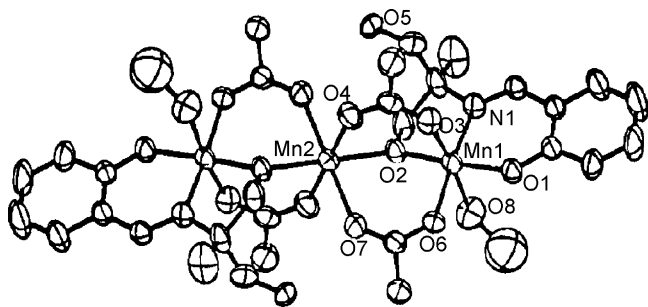
Fig. 22. ORTEP representation for α-Mn$^{II}$Mn$_2$$^{III}$(SALADHP)$_2$(OAc)$_4$ (CH$_3$OH)$_2$, **28** (figure was reproduced from Ref. [172], Copyright (1988) American Chemical Society and Ref. [174] (1989) Royal Society of Chemistry).



Fig. 25. Molecular structure of the anionic portion of [C$_2$H$_9$O$_2$]NaMn$_2$$^{III}$-(2-OH-SALPN)$_2$(OAc)$_4$] 2H$_2$O, **31**, from X-ray crystallography (figure was reproduced from Ref. [178], Copyright (1989) American Chemical Society).

of 129.45(6)° is permitted by the flexibility of the macrocyclic ligand.

Pecoraro and Kessissoglou also reported the observation of a $g = 2$ multiline signal from a DMF solution of the bent trinuclear, mixed valence manganese cluster β-[Mn$^{II}$Mn$_2$$^{III}$(SALADHP)$_2$(OAc)$_4$(CH$_3$OH)$_2$], **30** [173] (Fig. 24). Kessissoglou subsequently demonstrated that the interesting $g = 2$ multiline signal arose from a slight variant of this structure in which the terminal Mn$^{III}$ ions were five coordinate [176]. A comparable EPR active trinuclear Mn$_3$$^{II}$ complex [177] differed significantly in that it is a mixed-spin compound, not mixed-valence compound and exhibited a six-line rather than a multiline (>11 lines) feature at $g = 2$ seen in the Mn$_2$$^{II}$Mn$^{III}$ complex.

Since this report, several trinuclear complexes with Schiff base derivatives have been synthesized, typically resulting in weakly anti-ferromagnetically coupled complexes with an EPR signal at $g \approx 4$, indicating a $S = 3/2$ spin ground state [13]. Amongst these is the heterotrinuclear species [NaMn$_2$$^{III}$-(2-OH-SALPN)$_2$(OAc)$_4$]$^-$, **31** (Fig. 25), which was reported as the first cage structure providing complete encapsulation of an
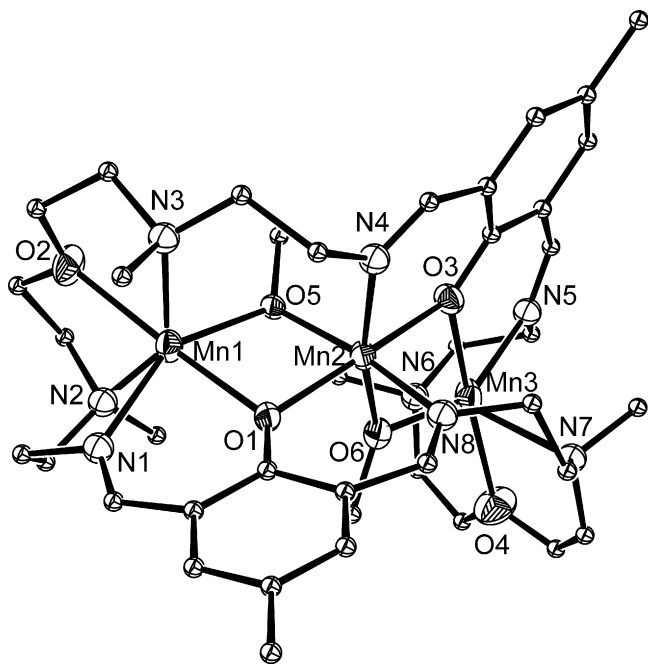


Fig. 23. ORTEP representations for the 7+ trinuclear complex, **29**, reported Asato and coworkers (figure was reproduced from Ref. [175], Copyright (2000) Royal Society of Chemistry).

enclose three manganese ions into its cavity [175]. Through spectroscopic and magnetic measurements the metal ion oxidation states were assigned as mixed valence Mn$_2$$^{II}$Mn$^{III}$ in the trinuclear complex, **29**, shown in Fig. 23 The Mn–Mn–Mn angle



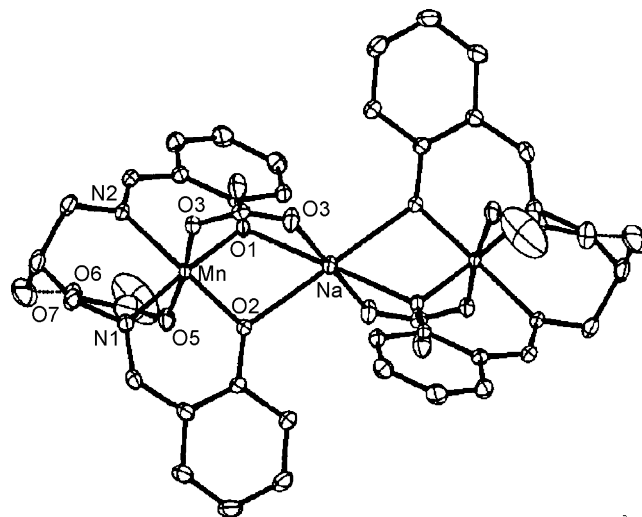Fig. 24. An ORTEP diagram of the bent structure in β-[Mn$^{II}$Mn$_2$$^{III}$(SALADHP)$_2$(OAc)$_4$(CH$_3$OH)$_2$], **30** (figure was reproduced from Ref. [173], Copyright (1989) Royal Society of Chemistry).

alkali-metal cation by bridging ligands in a discrete trinuclear formulation [178]. Probably the most important contribution from this molecule is the estimation of the very large zero field splitting parameter $D = -6.13\,cm^{-1}$ for $Mn^{III}$. This has been used as a benchmark both in the photosynthesis community and in the field of molecular magnets.

### 3.3.3. Models with three distinct oxidation levels

The assignment of the metal oxidation states of $S_0$ in the OEC has been quite controversial for over a decade. While there is general agreement that $S_1$ and $S_2$ correspond to $Mn_2^{III}Mn_2^{IV}$ and $Mn^{III}Mn_3^{IV}$, respectively, there has been an important question lingering as to whether $S_0$ corresponds to $Mn_3^{III}Mn^{IV}$ or $Mn^{II}Mn^{III}Mn_2^{IV}$. Resolution to this question is essential for fully understanding the mechanism of water oxidation since $S_0$ is the product state of the catalyst. While early assignments of the $S_0$ oxidation level came from EPR [179–181], one of the primary pieces of evidence supporting the $Mn^{II}Mn^{III}Mn_2^{IV}$ assignment is interpretation of the XANES spectrum of $S_0$ [182]. Proper interpretation of XANES spectroscopy requires appropriate small models. Unfortunately, there are only two structurally characterized compounds that contain Mn in more than two oxidation states and neither of these have been subjected to X-ray absorption analysis [183,184].

Very recently, Wieghardt and coworkers reported the synthesis of a novel mixed valent Mn trinuclear complex with the unique non-innocent ligand 2,4-di-*tert*-butyl-6-(2-(hydroxymethyl)phenylamino)phenol, H₃L [183]. This ligand can coordinate not only in its deprotonated form ($L_3^-$), but also in its oxidized *o*-iminobenzosemiquinonate ($L_2^{\bullet-}$) radical and *o*-iminobenzoquinone ($L_{IQ1}^-$) forms. This was first example of a trinuclear mixed-valent $Mn^{III}Mn^{II}Mn^{IV}$ complex, **32** (Fig. 26) that contains additionally two iminosemiquinone radicals, an iminobenzoquinone and a chloride ligand. All three forms of 2-aminophenol-based ligand were previously unambiguously characterized earlier in different compounds [185–192]. Proof

that several oxidation levels co-exist in this particular complex was evidenced not only by an X-ray structure determination but also by magnetic susceptibility experiments. The authors point out that the stability of such a complex supports the oxidation state assignment for the lower S-states of the OEC.

### 3.3.4. Use of XANES to probe multiple possible oxidation assignments in trinuclear compounds

Another relevant set of models would be compounds that have manganese ions separated in oxidation state by at least two oxidation levels. Of great interest are higher valent species, such as the $Mn^{II}Mn^{IV}Mn^{II}$ complex reported by Kessissoglou, Pecoraro and coworkers with the ligand 2,2′-dipyridyl ketonoxime ($pko^-$) **33**, shown in Fig. 27 [193]. This molecule contains a central $Mn^{IV}$, located on a crystallographic inversion center, flanked by two $Mn^{II}$ ions. The six bond distances around the central Mn atom average 1.91 Å, in good agreement with the average distance reported for mononuclear $Mn^{IV}$ compounds (e.g., $Mn^{IV}(SALADHP)_2$) and approximately 0.12 Å shorter than the average bond lengths that are typical for $Mn^{III}$ species. The lack of a Jahn–Teller distortion of the central Mn further supports the oxidation state assignment as $Mn^{IV}$ rather than $Mn^{III}$. The terminal Mn ions are coordinated to five nitrogen atoms and an oxygen atom with an average bond distance of 2.223 Å. This average value is typical for $Mn^{II}$ compounds and fully supports a valence trapped 2+ oxidation state for the terminal atoms. The best fit (for a model with $J_{12}$ being defined as the exchange parameter between the central $Mn^{IV}$ and terminal $Mn^{II}$ and $J_{22}$ set to 0) is $J_{12} = +6.13\,cm^{-1}$ and $g = 2.09$. The magnetic ground state, con-
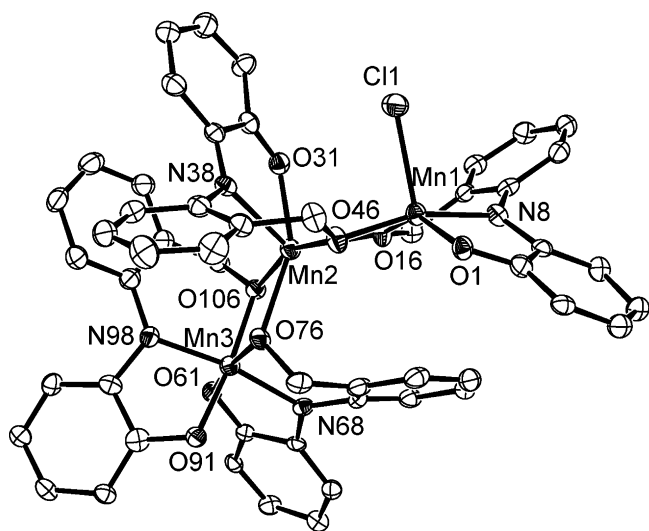


Fig. 26. ORTEP representation of $Mn^{III}Mn^{II}Mn^{IV}$ complex, **32**, reported by Wieghardt and coworkers (*t*-Bu groups removed for clarity) (figure was reproduced from Ref. [183], Copyright (2006) Royal Society of Chemistry).
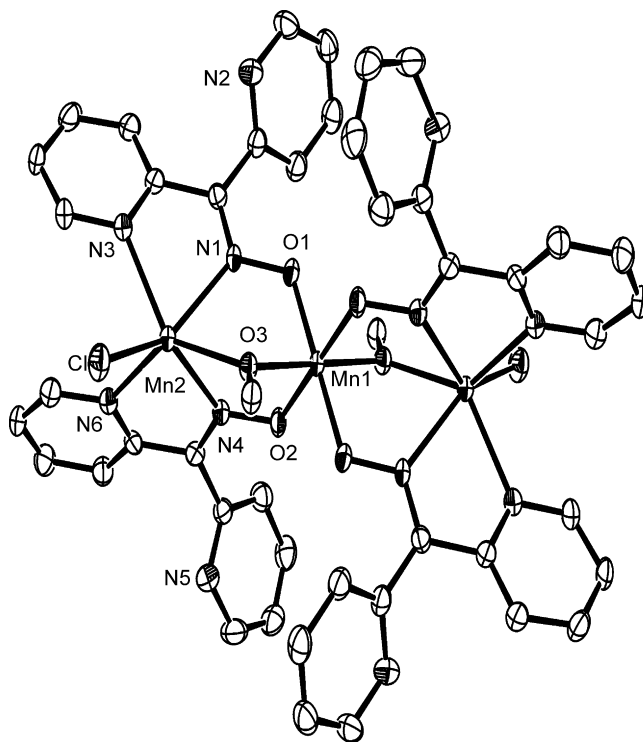


Fig. 27. ORTEP representation of $Mn^{II}Mn^{IV}Mn^{II}(pko)_4(CH_3O)_2(Cl)_2$, **33**, reported by Alexiou et al. (figure was reproduced from Ref. [193], Copyright (2003) Wiley–VCH Verlag GmbH & Co. KGaA).

(a)



(b)



Fig. 28. ORTEP representations of (a) $Mn^{III}Mn^{II}Mn^{III}(Hsaladhp)_2$ $(Sal)_4 \cdot 2CH_3CN$, **34** (figure was reproduced from Ref. [176], Copyright (2000) American Chemical Society), and (b) $Mn^{II}Mn^{IV}Mn^{II}(pko)_4(CH_3O)_2(SCN)_2$, **35** (figure was reproduced from Ref. [193], Copyright (2003) Wiley–VCH Verlag GmbH & Co. KGaA).
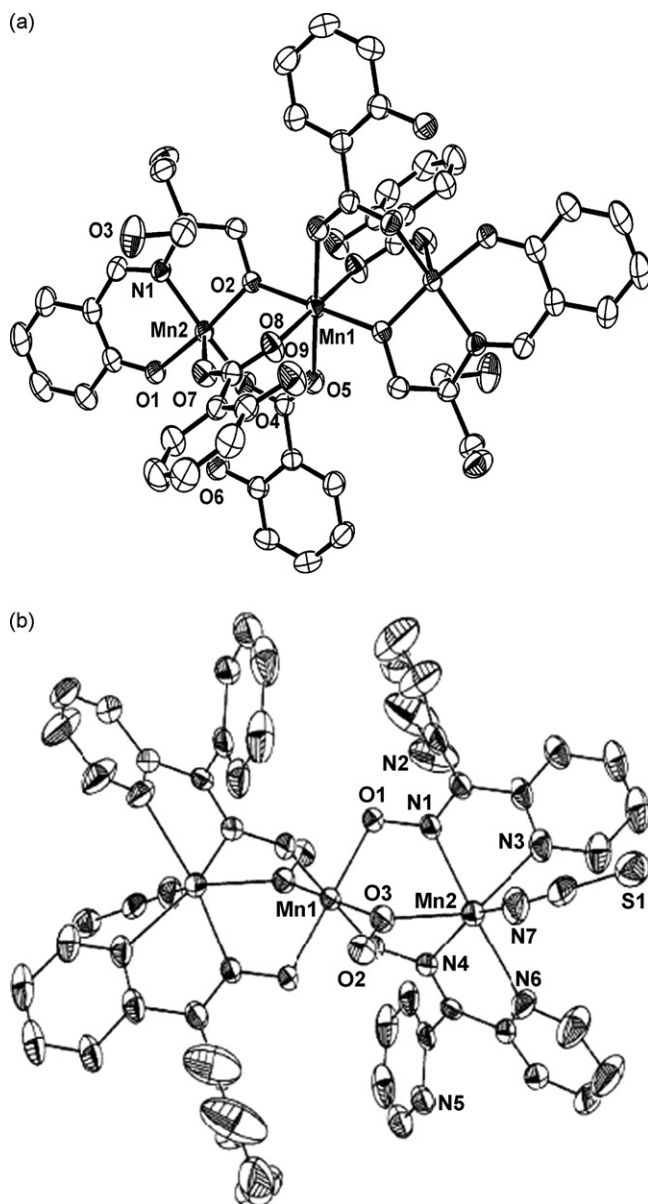
firmed by magnetization measurements at 4.5 K, is S = 13/2. A chloride analogue of this compound has also been prepared and characterized.

Comparative spectroscopic and magnetic studies between this $Mn^{II}Mn^{IV}Mn^{II}$ complex, **35**, and $Mn^{III}Mn^{II}Mn^{III}$ (**34**) compounds (shown in Fig. 28) have also been carried out [194]. The XANES spectra of both $Mn^{8+}$ complexes were fit with linear combinations of Mn model spectra. The best fit for the $Mn_2^{II}Mn^{IV}$ complexes gave an average oxidation state of 2.7, consistent both with the $Mn_2^{II}Mn^{IV}$ assignment and with the $Mn_2^{III}Mn^{II}$ alternative. The XANES spectrum for the authentic $Mn_2^{III}Mn^{II}$ trimer is somewhat narrower than for the $Mn_2^{II}Mn^{IV}$ compound and has a weaker 1s–3d transition (Fig. 29). This



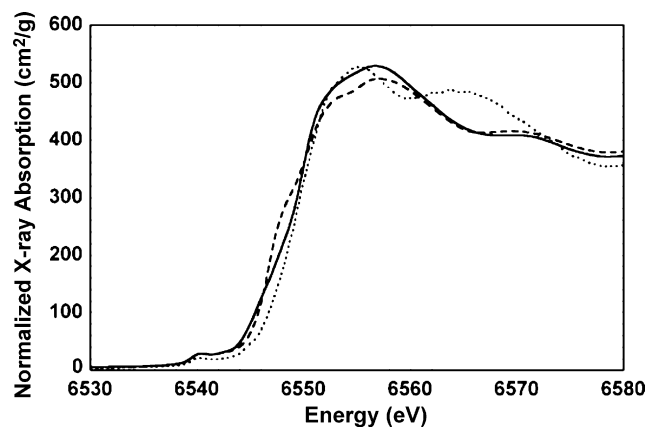Fig. 29. XANES spectra of $Mn_2^{II}Mn^{IV}$ (solid and dashed lines) and $Mn_2^{III}Mn^{II}$ (dotted line) (figure was reproduced from Ref. [194], Copyright (2003) American Chemical Society).

difference in XANES shape suggested that it was possible to distinguish experimentally between the two valence configurations. When the XANES spectra for the $Mn_2^{II}Mn^{IV}$ were fit with a linear combination of $Mn^{II}$, $Mn^{III}$, and $Mn^{IV}$, the best fits all had less than 15% $Mn^{III}$, while the corresponding fits for the $Mn_2^{III}Mn^{II}$ compound never gave more than 15% $Mn^{IV}$, consistent in both cases with the proposed oxidation state assignments. Similarly, fits of $Mn_2^{II}Mn^{IV}$ using a linear combination of $Mn^{II}$ and $Mn^{IV}$ models were ca. 50% better than fits using a linear combination of $Mn^{II}$ and $Mn^{III}$. Comparable behavior was seen for $Mn_2^{III}Mn^{II}$, where fits using $Mn^{II}$ plus $Mn^{III}$ were ca. 70% better. These data suggested that XANES spectroscopy, at least when three Mn ions are involved, would be capable of correctly determining the oxidation states of Mn in $S_0$. Furthermore, these studies confirm that a biological cluster rich in oxy-anions at one site and containing neutral nitrogen donors at another site can allow a stable $Mn^{II}/Mn^{IV}$ mixed valency.

### 3.3.5. $Mn_3^{IV}$ clusters

Wieghardt and coworkers were among the first to employ functionalized 1,4,7-triazacyclononane (TACN) ligands for



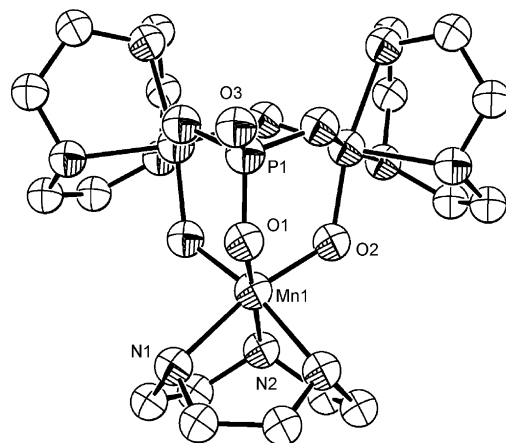Fig. 30. ORTEP representation of the cation $[L_3Mn_3(\mu\text{-}O)_3(\mu\text{-}PO_4)]^{3+}$ of the adamantane-like cluster, **36**, reported by Wieghardt and coworkers (figure was reproduced from Ref. [195], Copyright (1988) Royal Society of Chemistry).
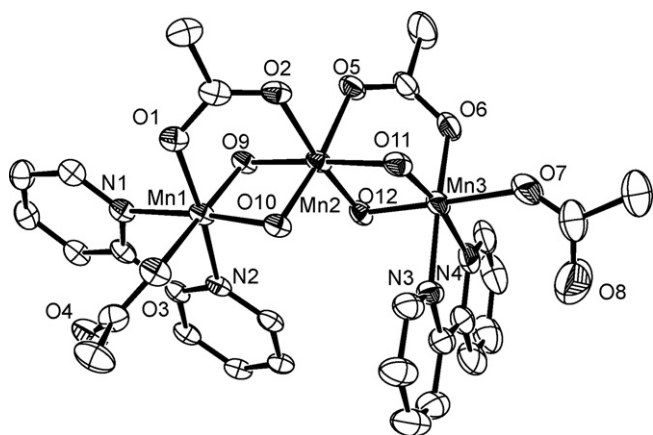
Fig. 31. ORTEP representation of a $Mn_3^{IV}$ trinuclear structure, **37**, reported by Christou and coworkers (figure was reproduced from Ref. [196], Copyright (2002) Royal Society of Chemistry).

complexes with $Mn_3^{IV}$ clusters [195]. The metal ions in these complexes, which resulted in adamantane-like arrangements, are connected by one $\mu_3$-$XO_4$ (X = P, As, or $V^V$) and three bridging $\mu_2$-oxo groups. The crystal structure of the phosphate analogue, **36** (Fig. 30) was reported. The short Mn–$O_{oxo}$ bond lengths of ca. 1.785 Å are typical of $Mn^{IV}$–O–$Mn^{IV}$ units. Replacement of Ca(II) for P(V) would begin to resemble the present models for the OEC structure, although the compound would still need to be converted from an adamantane structural type to a pseudocubane.

Christou and coworkers recently reported an open structure trinuclear $Mn_3^{IV}$ complex, **37** (Fig. 31) comprised of bent $Mn_3O_4$ unit, analogous to many proposed structures for the OEC

[196]. A bis($\mu_2$-oxo)($\mu_2$-acetato) bridging motif connects the central Mn to the terminal metal centers, which are capped by bipyridine and acetate ligands. The metric parameters were typical for those usually observed in $Mn^{IV}$ complexes. The central metal is solely coordinated by oxygen donors, which may lead to an increased stability of this high valent cluster.

## 3.4. Tetranuclear Mn complexes

A variety of tetranuclear clusters with oxidation states ranging from $Mn_4^{II}$ to $Mn_4^{IV}$ have been prepared [6,7,13]. A recent search of the Cambridge Structural Database (CSD) revealed over 150 ($\mu$-O)$Mn_4$ complexes that have been structurally characterized. Fig. 32 shows the commonly observed cluster types found in tetranuclear Mn-oxo cores [92]. As the OEC has at most only one $Mn^{II}$ ion in the $S_0$ state of the Kok cycle, we will focus our discussion by disregarding those models composed primarily of $Mn^{II}$ ions. A number of studies have been devoted to isolating such clusters, with the overall aim being the oxidation to more relevant models [197–199]. Unfortunately, many of these complexes have not been shown to access the higher valencies needed to accurately mimic the $Mn_4Ca$ cluster of the OEC. Consequently, in this discussion we will focus primarily on complexes with average Mn oxidation states of 3.0 or greater.

### 3.4.1. Adamantane-like structures

Since the initial report in 1983 by Wieghardt and coworkers [200]. there have been five additional crystallographic reports of the adamantane shaped $Mn_4O_6$ complex, **38** (Fig. 33) with the 1,4,7-triazacyclononane (TACN) ligand [122,201–203]. This complex was originally prepared by mixing aqueous alkaline
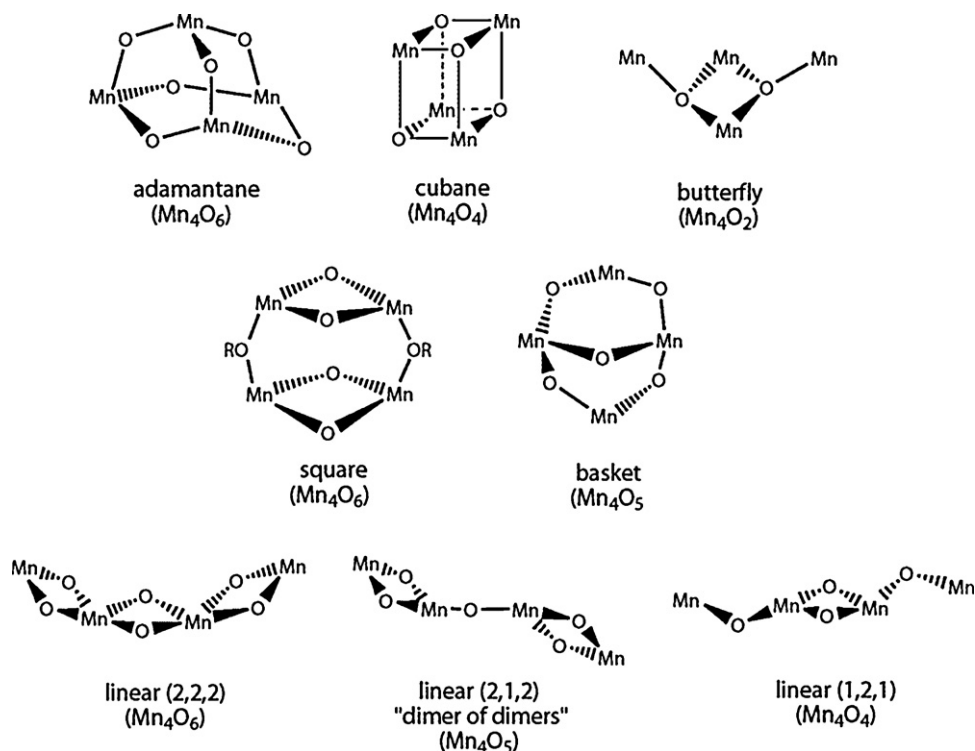


Fig. 32. Different core types observed in Mn-oxo tetramers (figure was reproduced from Ref. [92], Copyright (2005) American Chemical Society).
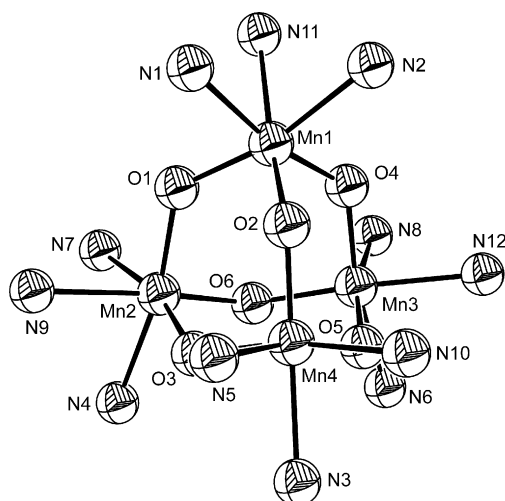
Fig. 33. ORTEP representation of the $Mn_4O_6$ complex with the TACN ligand first reported by Wieghardt and coworkers, **38** (figure was reproduced from Ref. [200], Copyright (1983) Wiley–VCH Verlag GmbH & Co. KGaA).

solutions of TACN with $MnCl_2$ under oxygen to produce black solutions, which yielded black crystals of the product after addition of NaBr. The tetranuclear $Mn^{IV}$ assignment was made based on results of X-ray crystallographic analysis and magnetic measurements. A search of the CSD reveals that half of the tetranuclear adamantane-shaped Mn-oxo clusters are salts of the $TACN_4Mn_4O_6$ structure originally reported by Wieghardt and coworkers. Armstrong and coworkers have also prepared several adamantane-shaped tetranuclear complexes [204].

### 3.4.2. Linear structures

In 1989, Armstrong and coworkers reported the first of several tetranuclear model complexes from their group. The complex $\{[Mn_2(TPHPN)(O_2CCH_3)(H_2O)]_2O\}^{4+}$, **39**, has an average Mn oxidation state of 2.5 and is believed to be a $Mn_2^{II}Mn_2^{III}$ system [205]. A year later they reported the linear complex, $[Mn_4O_2(TPHPN)_2(H_2O)_2(CF_3SO_3)_2]^{3+}$, **40** (Fig. 34) which has an average Mn oxidation state of 2.75 [184]. An assignment of

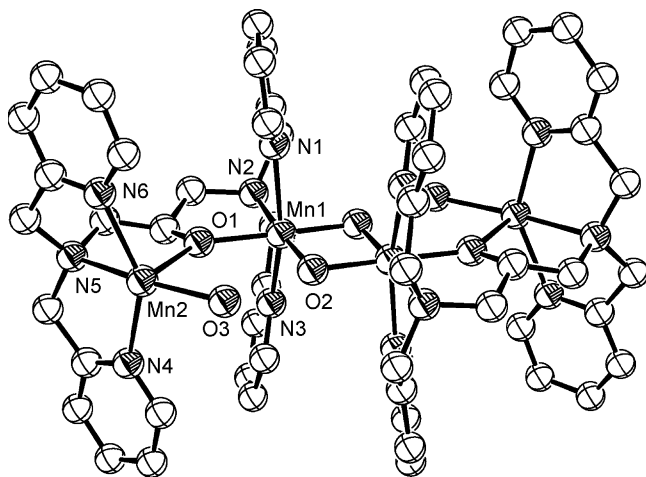$Mn^{II}Mn^{III}Mn^{IV}Mn^{II}$ was made based on the bond distances in the crystal structure and the electronic spectrum in acetonitrile, which, in the visible region, closely resembles other species that contain the $(Mn_2O_2)^{3+}$ core [116]. Several important criteria for a synthetic analogue of the OEC manganese center are met with this complex. As is the case with most high valent di-μ-oxo dimers, it has a 2.7 Å Mn···Mn separation, a value which is the hallmark of the OEC. One nice feature of the complex is that it contains coordinated water molecules. The feature of greatest interest is the mixed valency assignment. This compound was the first structure to show manganese in three different oxidation states and, hence, serves as an excellent model for $S_0$. This compound demonstrated for the first time that $Mn^{II}$ and $M^{IV}$ could be stable to comproportionation within the same molecule, especially noteworthy given that there is a single atom alkoxo oxygen atom connecting these two ions.

### 3.4.3. XANES to probe multiple possible oxidation assignments in tetranuclear compounds

More recent efforts to synthesize tetranuclear Mn complexes as biomimetic models have yielded several discrete species that have a total Mn formal charge of +10. In 2002, Kessissoglou and coworkers reported the synthesis of a mixed-valent $Mn_3^{II}Mn^{IV}$ complex, **41**, with a μ4-O bridge to the four Mn ions (Fig. 35) [206]. This compound is another rare example of $Mn^{II}$ and $Mn^{IV}$ within the same cluster. This complex most resembles the "basket" variety shown in Fig. 32, although with only one μ4-oxo (rather than μ2) and with the hydroxamate ligands bridging the metals in addition to the bulky carboxylates. Comparison of the FTIR spectrum of this compound with a Zn metallacrown complex, $[Zn_4(OH)_2(pko)_4Cl_2]$ suggests that there is no additional band that may be due to a Mn=O bond. Variable temperature



Fig. 34. ORTEP representation of $[Mn_4O_2(TPHPN)_2(H_2O)_2(CF_3SO_3)_2]^{3+}$, **40** (triflate counter anions not shown for clarity) (figure was reproduced from Ref. [184], Copyright (1990) American Chemical Society).
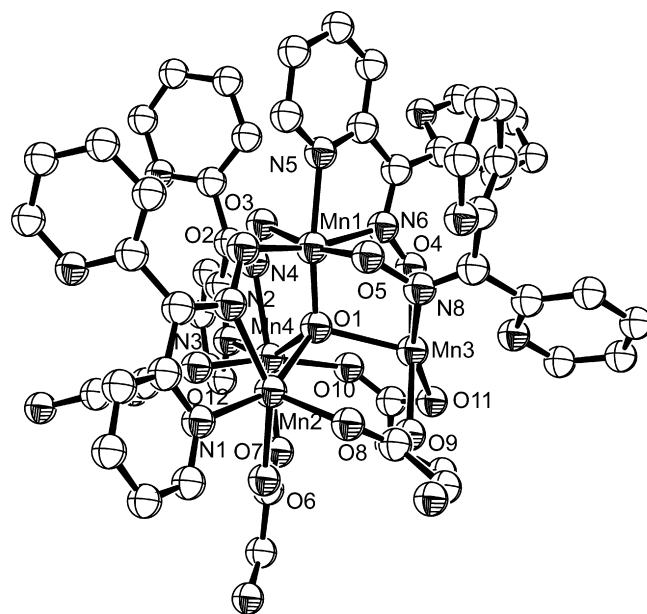


Fig. 35. ORTEP representation of the tetranuclear cluster $Mn_3^{II}Mn^{IV}$ complex, **41** (figure was reproduced from Ref. [206], Copyright (2002) Wiley–VCH Verlag GmbH & Co. KGaA).

magnetic experiments were used to support the $Mn^{IV}$ assignment of Mn1.

Building on earlier work with trinuclear complexes, Pecoraro and coworkers have most recently prepared tetranuclear complexes that are valence isomers [207]. X-ray absorption spectroscopy is being utilized to set a standard for reliably discerning the Mn oxidation states in tetranuclear cluster compounds. In this case, the comparison is between $Mn^{10+}$ complexes with formal oxidation state assignments of either $Mn_3^{II}Mn^{IV}$ (complex **41**, shown in Fig. 35) or $Mn_2^{II}Mn_2^{III}$ [180]. As in earlier studies of $Mn_3^{8+}$ complexes [193], the correct average oxidation state may be attained within the estimated uncertainty of $\sim\pm0.25\,eV$, although differences between these valence isomers is larger than previously seen.

Based on XAS and EPR studies, a $Mn^{II}Mn^{III}Mn_2^{IV}$ assembly has been suggested for the tetranuclear Mn cluster in $S_0$. The existence of three different Mn oxidation states in the same complex is exceptional. Under most circumstances, $Mn^{II}$ and $Mn^{IV}$ would comproportionate to give a $Mn_4^{III}$ species; however, the model chemistry of Armstrong [184], Kessissoglou and coworkers [193,194], and Wieghardt et al. [183] has demonstrated that $Mn^{II}$ and $Mn^{IV}$ can exist in the same molecule with single atom bridges. This suggests that the OEC would be capable of stabilizing multiple Mn oxidation states in the same cluster and that XANES spectroscopy can distinguish correctly $Mn^{II}Mn^{III}Mn_2^{IV}$ and $Mn_3^{III}Mn^{IV}$ formulations for the enzyme.

The average Mn oxidation states +3.25 and +3.50 are considered to be favorable for models of the $S_1$ state of the OEC. The compounds $(H_2Im)_2[Mn_4O_3Cl_6(MeCOO)_3(HIm)]$, $[Mn_4O_3Cl_4(MeCOO)_3(py)_3]$, and $[Mn_4O_3Cl(MeCOO)_3(dbm)_3]$ (HIm = imidazolium) which have a distorted cubane $[Mn_4O_3Cl]$ core with a $(\mu_3\text{-}O)Mn_3$ bridging group [208–210] represent the formulation of $Mn_3^{III}Mn^{IV}$. Meanwhile, the $[(Mn_2O_2)_2(tphpn)_2]^{4+}$ cation with a $(\mu\text{-}O)Mn_2$ bridging unit [101,113,211] is an example of a $Mn_2^{III}Mn_2^{IV}$ assignment. Average Mn oxidation states of +3.75 with a $Mn^{III}Mn_3^{IV}$ formulation, the most favorable for the $S_2$ state, and +4.00 for $Mn_4^{IV}$ have been reported for the $[Mn_4O_6(bpy)_6]^{3+}$ and $[Mn_4O_6(bpy)_6]^{4+}$ ions, respectively [212].

### 3.4.4. Cuboidal models

Dismukes and coworkers have reported several $Mn_4O_x$ cluster compounds with cuboidal type structural arrangements [160,213–217]. An example of such a complex, **42**, is shown
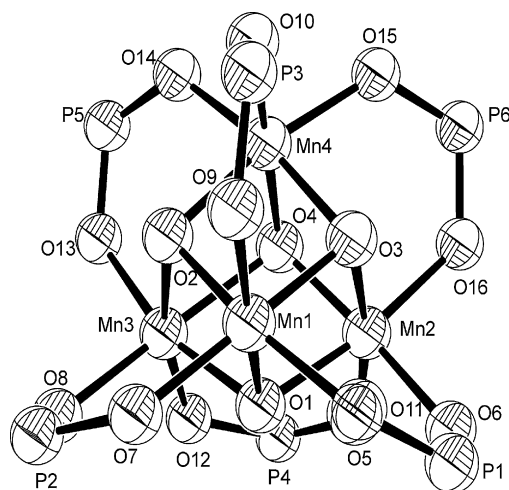


Fig. 36. ORTEP representation of complex, **42**, reported by Dismukes and coworkers, with anisole rings omitted for clarity (figure was reproduced from Ref. [217], Copyright (2006) American Chemical Society).

in Fig. 36, where the Mn3 ion was assigned a 3+ oxidation state due to Jahn–Teller distortions revealed by XRD with all the other Mn ions assigned as $Mn^{IV}$ [217]. These compounds reportedly undergo photo-rearrangement to release $O_2$ (and a diarylphosphinate ligand) to yield a butterfly type product (Scheme 5) [214,216]. From these data the authors have suggested a similar route for water oxidation by PSII that produces $O_2$ by the coupling of two bridging oxides of the cluster. Christou and coworkers have also reported a number of cluster compounds that have either cuboidal [208,209] or butterfly [218] motifs.

Several issues hamper such complexes as effective biomimetic models. First, the diarylphosphinate ligands are unlikely to serve as the most relative models for the protein encasing the $Mn_4O_xCa$ cluster. Secondly, such models do not adequately account for the role of a Ca ion or the dangler Mn ion found in the recent crystallographic reports. Finally, it appears that the "butterfly" product complexes are dead-ends and no catalytic activity has yet been demonstrated with such compounds.

### 3.4.5. Models for dimer-of-dimers hypothesis

As numerous examples of tetranuclear Mn complexes are amassed, there becomes a greater need to focus on only models that are relevant to PSII. Although the dimer-of-dimers model has fallen out of favor with many researchers, there
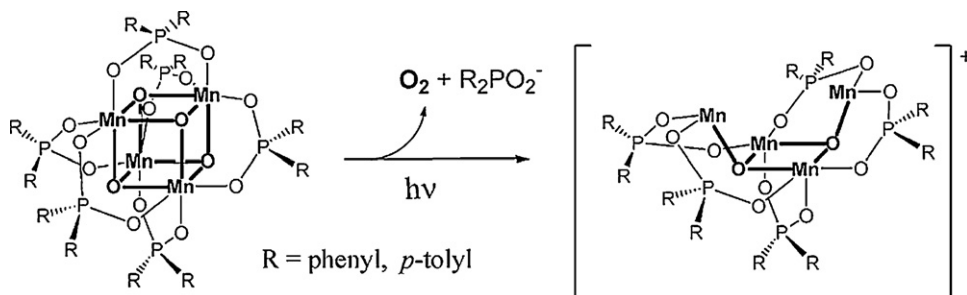


Scheme 5. Proposed $O_2$ production (along with release of diarylphosphinate) by photo-induced rearrangement of the $[Mn_4O_4]^{6+}$ "cubane" core to a $[Mn_4O_2]^{6+}$ "butterfly" core (figure was reproduced from Refs. [214,216], Copyrights (2000) American Chemical Society and (2002) Springer).

remains a genuine need to study models that mimic such archi-tectures. In the early 1990s, Girerd and coworkers reported a model complex, $[Mn_4O_6(bpy)_6]^{4+}$, that is composed of two di-$\mu$-oxo-dimanganese units linked by a di-$\mu$-oxo bridge [219]. Recently, Brudvig and coworkers have offered two alternative linear topologies using $Mn_4^{IV}(terpy)$ complexes with different combinations of a mono-$\mu_2$-oxo and bis-$\mu_2$-oxo-bridged Mn units [91,92]. They suggested that these linear (2, 1, 2) and (1, 2, 1) bridged complexes as synthetic examples for the dimer of dimers model for the OEC. Complex **43**, which has 2 bis-$\mu_2$-

oxo bridges connecting the terminal Mn to the inner ones and a mono $\mu$-oxo bridge connecting the central $Mn^{IV}$ ions, is shown at left in Fig. 37. The related complex, **44**, is shown in Fig. 37, right. The most noteworthy feature of the (1,2,1) complex **44** is the ligation of all three types of water-derived ligands (aqua, hydroxo, and oxo) to the terminal $Mn^{IV}$ ions of this tetrameric Mn complex, which the authors claimed was the first known example of such ligation.

## 4. Mechanistic proposals

Given all of the information obtained from biophysical stud-ies of the OEC and characterization of model compounds, we may begin to piece together a combined structural and mech-anistic model for the OEC. Because the rest of this thematic issue focuses on numerous mechanistic proposals, we will not re-describe these various models here. Instead, we will focus our attention on a structural and mechanistic model that we described in 1997, first for the dimer of dimers structure [143] and then in 2000 using the 3 + 1 cluster formulation [10].

As we discussed with Fig. 14, analysis of magnetic and EPR spectral data led to a structure that generally predicted the struc-tures which we are presently using to interpret the chemistry of this system. We can now move a step forward with this generalized model and begin to assess the function of each of the components of this $Mn_4Ca$ cluster. The model presented in Fig. 38 shows a diagrammatic representation of the $Mn_4Ca$ clus-ter that presents possible functions of the cluster. To interpret this structure we will use an oxidation state assignment for $S_0$ equal to $Mn^{II}Mn^{III}Mn_2^{IV}$ and for $S_4$ an oxidation level of $Mn_3^{IV}Mn^V$. It is well known that the Mn cluster is unstable, especially in $S_0$ and that the redox active tyrosine $Y_D^+$ can oxidize $S_0$ to $S_1$ [220]. This may be Nature's way of stabilizing the cluster in the
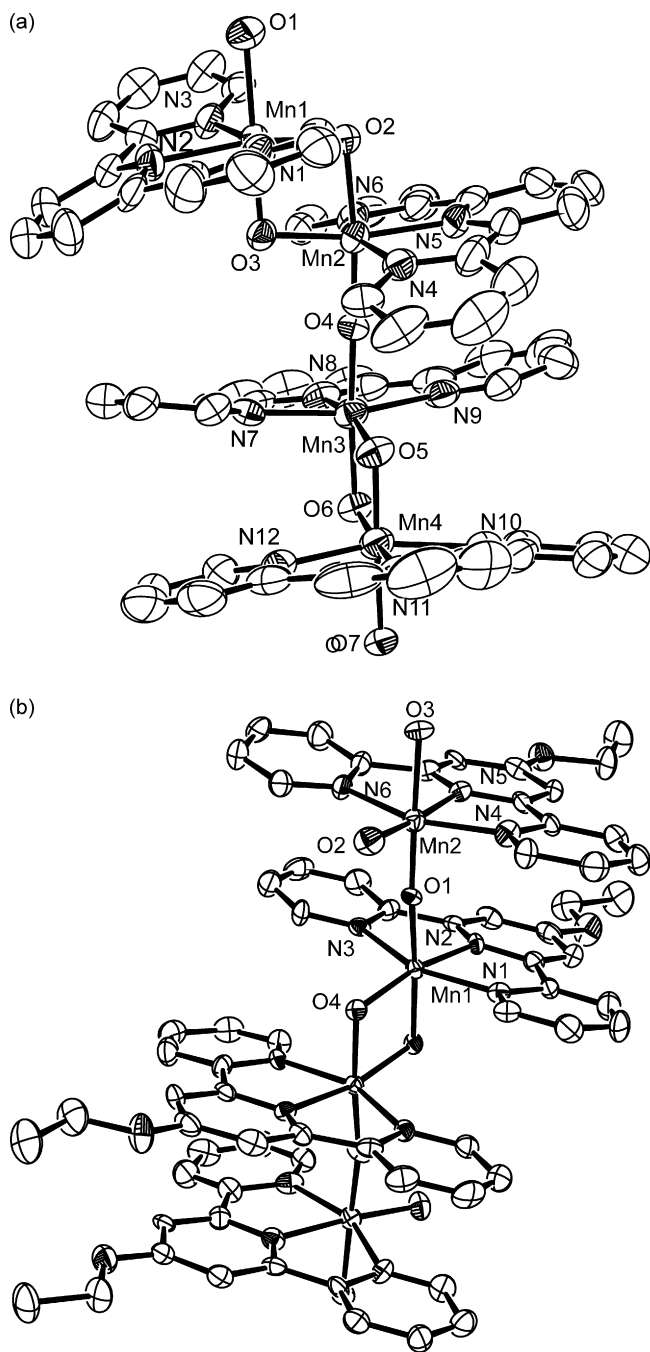


Fig. 37. ORTEP representations of the tetranuclear Mn(terpy) complexes: (a) **43** and (b) **44** (figures reproduced from Refs. [91,92], Copyrights (2004 and 2005) American Chemical Society).
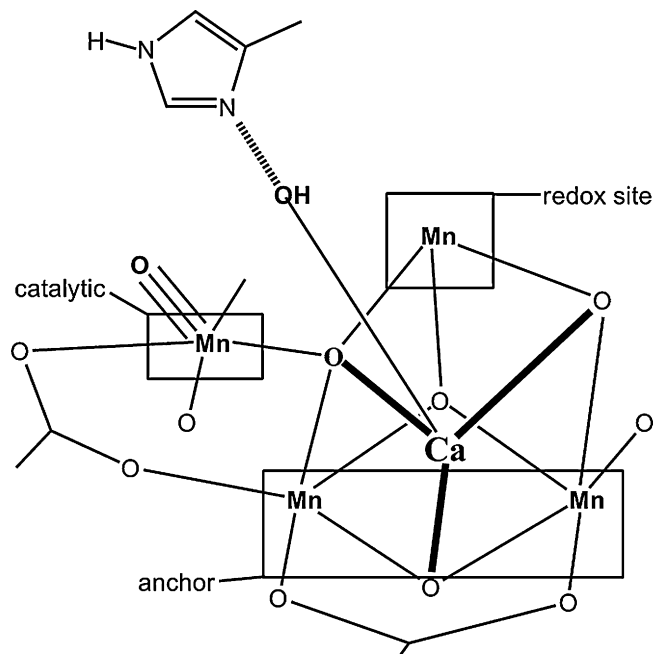


Fig. 38. Structural model for $Mn_4Ca$ cluster with proposed functional roles of Mn and Ca ions.

lowest S-state, since the $Mn^{II}$ has both low stability and rapid kinetics, which could lead to cluster decomposition. Oxidizing $S_0$ to $S_1$ would remove any $Mn^{II}$ from the cluster. However, if $Mn^{II}$ is essential for the oxidation process, how can one transiently stabilize this cluster? One way would be to incorporate a highly stable $Mn^{IV}(\mu_2\text{-O})_2$ core which is both thermodynamically and kinetically stable. Consistent with this idea, Yocum has demonstrated that two of the manganese ions in the cluster can be reduced by reductants such as hydroxylamine, whereas two others are susceptible to bulkier hydroquinone reductants [221]. This might support the notion that there are two special manganese ions that do not change oxidation state through the process of cluster photo-oxidation. We designate these as the anchor Mn ions which are spatially removed from the catalytic centers.

In order to oxidize water, the enzyme must accumulate four oxidizing equivalents. However, even an oxidation of a single manganese ion from the $Mn^{II}$ to $Mn^{V}$ oxidation level only accumulates three oxidizing equivalents. Therefore, another manganese ion is required to be oxidized in order to store the fourth oxidizing equivalent. If the catalytic center which goes from $Mn^{II}$ to $Mn^{V}$ is indeed the dangler manganese, we can then envision the trinuclear portion of the $Mn_4Ca$ cluster as a coupled trinuclear redox co-factor making its function in some ways similar to the trinuclear Cu cluster in ascorbate oxidase [222]. Thus, one of the remaining Mn ions serves as a storage site for the fourth redox equivalent while the last manganese, the dangler, serves as the main catalytic site.

This model accounts for the function of the four manganese ions, but alone, these centers still would be incapable of water oxidation. Even if the $Mn^{II}$ aqua ion of $S_0$ is oxidized to $Mn^{V}=O$ in $S_4$, one still needs a source of another oxygen atom. This atom could, of course, originate from water bound to the redox manganese; however, a more satisfying hypothesis is that the $Ca^{II}$ does not simply stabilize the cluster, but instead plays a vital catalytic role [143]. In this case, a water bound to $Ca^{II}$ is deprotonated to form minimally a $Ca^{II}$–OH and possibly a strongly hydrogen bonded Ca–O which is reminiscent of the $Mn^{IV}$–O of Borovik's compound [79]. This highly nucleophilic oxide could attack a proximate $Mn^{V}=O$ leading to the formation of an O–O bond and, ultimately, dioxygen.

This water oxidation mechanism was proposed by Pecoraro in the late 1990s [143]. Subsequently, Brudvig and coworkers have beautifully elaborated on these ideas to generate a unified mechanism that accounts for the detailed behavior of the OEC across the S cycle [15,223–225]. This proposal is shown as Fig. 38. For the latest perspective on this detailed process, the interested reader is referred to Brudvig's review in this issue.

Another important mechanism that drove much of the thinking in this field was proposed by Babcock and coworkers [226]. The basis of their ideas was that H-atom abstraction was a key mechanistic event which led to the formation of a $Mn^{IV}=O$ in $S_3$ that could couple to a $Mn^{IV}=O$ generated during the $S_3 \rightarrow S_4 \rightarrow S_0$ transition. While intellectually stimulating, we showed using XANES spectroscopy that this mechanism was not viable [49].

Recently, Dau has examined the immediate aftermath of oxidation from $S_3$ to $S_4$ and also shown that there is no evidence for either $Mn^{IV}=O$ or $Mn^{V}=O$ [227]. Dau describes the period between the initial photo-oxidation and the chemistry of water oxidation as $S_4$ and the subsequent period as $S_4'$. Unfortunately, the critical chemistry in this model occurs in $S_4'$, therefore, we still do not know whether the manganyl exist transiently during the water oxidation process. At present our proposal appears consistent with the majority of data. The biggest tests which this process must overcome in the future are determining whether Mn oxidation does occur from $S_2 \rightarrow S_3$ and whether $S_0$ is $Mn^{II}Mn^{III}Mn_2^{IV}$ or $Mn_3^{III}Mn^{IV}$. Thus, these are some of the most important issues that need to be resolved in future biophysical and modeling studies.

## 5. Conclusion

In this monograph, we have investigated the chemistry of photosynthesis from the perspective of contributions made by small molecule model compounds. We have shown that over the past thirty years, models have been essential for laying a foundation for the understanding of manganese over several oxidation states and in structures of varying nuclearities. Even in recent years, models have been important for testing various proposals for water oxidation. The eventual hope is that true biomimetic chemistry leading to small molecule water oxidation catalysis can occur. Only in this way are we likely to test different proposals for water oxidation. In addition, water oxidation chemistry has garnered greater importance as the oxidizing half of a "Hydrogen Economy". To ecologically and economically burn $H_2$, using $O_2$, one should couple hydrogen production to dioxygen production from water. When such catalytic advances are made, we will not only have conquered one of the most challenging chemical reactions in nature, but also have taken a step toward generating new energy sources to sustain our civilization.

## Acknowledgment

## References

[1] B. Kok, B. Forbush, M. McGloid, Photochem. Photobiol. 11 (1970) 457.
[2] P. Joliot, A. Joliot, Biochim. Biophys. Acta 305 (1973) 302.
[3] P. Joliot, Brookhaven Symposia Biol. (1966) 418.
[4] P. Joliot, Biochim. Biophys. Acta 102 (1965) 116.
[5] V.L. Pecoraro, Photochem. Photobiol. 48 (1988) 249.
[6] K. Wieghardt, Angew. Chem. Int. Ed. Engl. 28 (1989) 1153.
[7] V.L. Pecoraro, M.J. Baldwin, A. Gelasco, Chem. Rev. 94 (1994) 807.
[8] R. Manchanda, G.W. Brudvig, R.H. Crabtree, Coord. Chem. Rev. 144 (1995) 1.
[9] C. Tommos, G.T. Babcock, Acc. Chem. Res. 31 (1998) 18.
[10] V.L. Pecoraro, W.Y. Hsieh, in: Metal Ions in Biological Systems, vol. 37, 2000, p. 429.
[11] M. Yagi, M Kaneko, Chem. Rev. 101 (2001) 21.
[12] G.M. Ananyev, L. Zaltsman, C. Vasko, G.C. Dismukes, Biochim. Biophys. Acta: Bioenerg. 1503 (2001) 52.

[13] S. Mukhopadhyay, S.K. Mandal, S. Bhaduri, W.H. Armstrong, Chem. Rev. 104 (2004) 3981.

[14] A.J. Wu, J.E. Penner-Hahn, V.L. Pecoraro, Chem. Rev. 104 (2004) 903.

[15] J.P. McEvoy, G.W. Brudvig, Chem. Rev. 106 (2006) 4455.

[16] K.N. Ferreira, T.M. Iverson, K. Maghlaoui, J. Barber, S. Iwata, Science 303 (2004) 1831.

[17] J. Barber, K. Ferreira, K. Maghlaoui, S. Iwata, Phys. Chem. Chem. Phys. 6 (2004) 4737.

[18] B. Loll, J. Kern, W. Saenger, A. Zouni, J. Biesiadka, Nature 438 (2005) 1040.

[19] J. Yano, J. Kern, K.D. Irrgang, M.J. Latimer, U. Bergmann, P. Glatzel, Y. Pushkar, J. Biesiadka, B. Loll, K. Sauer, J. Messinger, A. Zouni, V.K. Yachandra, Proc. Natl. Acad. Sci. U.S.A. 102 (2005) 12047.

[20] J. Yano, J. Kern, K. Sauer, M.J. Latimer, Y. Pushkar, J. Biesiadka, B. Loll, W. Saenger, J. Messinger, A. Zouni, V.K. Yachandra, Science 314 (2006) 821.

[21] P.S. Pavacik, J.C. Huffman, G.J. Christou, J. Chem. Soc. Chem. Commun. (1986) 43–44.

[22] D.P. Kessissoglou, W.M. Butler, V.L. Pecoraro, J. Chem. Soc. Chem. Commun. (1986) 1253.

[23] D.P. Kessissoglou, X.H. Li, W.M. Butler, V.L. Pecoraro, Inorg. Chem. 26 (1987) 2487.

[24] T.M. Rajendiran, J.W. Kampf, V.L. Pecoraro, Inorg. Chim. Acta 339 (2002) 497–502.

[25] B. Adam, E. Bill, E. Bothe, B. Goerdt, G. Haselhorst, K. Hildenbrand, A. Sokolowski, S. Steenken, T. Weyhermüller, K. Wieghardt, Chem. Eur. J. 3 (1997) 308.

[26] O. Hansson, R. Aasa, T. Vanngard, Biophys. J. 51 (1987) 825.

[27] E. Pedersen, H. Toftlund, Inorg. Chem. 13 (1974) 1603.

[28] S. Pal, P. Ghosh, A. Chakravorty, Inorg. Chem. 24 (1985) 3704.

[29] J.C. Hempel, L.O. Morgan, W.B. Lewis, Inorg. Chem. 9 (1970) 2064.

[30] K.D. Magers, C.G. Smith, D.T. Sawyer, Inorg. Chem. 19 (1980) 492.

[31] D.T. Richens, D.T. Sawyer, J. Am. Chem. Soc. 101 (1979) 3681.

[32] K.L. Brown, R.M. Golding, P.C. Healy, K.J. Jessop, W.C. Tennant, Aust. J. Chem. 27 (1974) 2075.

[33] S.K. Chandra, P. Basu, D. Ray, S. Pal, A. Chakravorty, Inorg. Chem. 29 (1990) 2423.

[34] G.C. Yin, J.M. McCormick, M. Buchalova, A.M. Danby, K. Rodgers, V.W. Day, K. Smith, C.M. Perkins, D. Kitko, J.D. Carter, W.M. Scheper, D.H. Busch, Inorg. Chem. 45 (2006) 8052.

[35] S.N. Poddar, N.G. Podder, Indian J. Chem. 6 (1968) 276.

[36] G.C. Yin, M. Buchalova, A.M. Danby, C.M. Perkins, D. Kitko, J.D. Carter, W.M. Scheper, D.H. Busch, Inorg. Chem. 45 (2006) 3467.

[37] G. Yin, A.M. Danby, D. Kitko, J.D. Carter, W.M. Scheper, D.H.J. Busch, Am. Chem. Soc. 129 (2007) 1512.

[38] S.M. Saadeh, M.S. Lah, V.L. Pecoraro, Inorg. Chem. 30 (1991) 8.

[39] D.H. Kim, R.D. Britt, M.P. Klein, K.J. Sauer, Am. Chem. Soc. 112 (1990) 9389.

[40] R.D. Britt, J.L. Zimmermann, K. Sauer, M.P.J. Klein, Am. Chem. Soc. 111 (1989) 3522.

[41] T.J. Collins, S.W. Gordon-Wylie, J. Am. Chem. Soc. 111 (1989) 4511.

[42] F.C. Anson, T.J. Collins, T.G. Richmond, B.D. Santarsiero, J.E. Toth, B. Treco, J. Am. Chem. Soc. 109 (1987) 2974.

[43] T.J. Collins, R.D. Powell, C. Slebodnick, E.S. Uffelman, J. Am. Chem. Soc. 112 (1990) 899.

[44] C.G. Miller, S.W. Gordon-Wylie, C.P. Horwitz, S.A. Strazisar, D.K. Peraino, G.R. Clark, S.T. Weintraub, T.J. Collins, J. Am. Chem. Soc. 120 (1998) 11540.

[45] K. Srinivasan, P. Michaud, J.K. Kochi, J. Am. Chem. Soc. 108 (1986) 2309.

[46] W. Zhang, J.L. Loebach, S.R. Wilson, E.N. Jacobsen, J. Am. Chem. Soc. 112 (1990) 2801.

[47] R. Irie, K. Noda, Y. Ito, T. Katsuki, Tetrahedron Lett. 32 (1991) 1055.

[48] T. Collins, J. Acc. Chem. Res. 35 (2002) 782.

[49] T.C. Weng, W.Y. Hsieh, E.S. Uffelman, S.W. Gordon-Wylie, T.J. Collins, V.L. Pecoraro, J.E. Penner-Hahn, J. Am. Chem. Soc. 126 (2004) 8070.

[50] F.M. Macdonnell, N.L.P. Fackler, C. Stern, T.V. Ohalloran, J. Am. Chem. Soc. 116 (1994) 7431.

[51] N.L.P. Fackler, S. Zhang, T.V. O'Halloran, J. Am. Chem. Soc. 118 (1996) 481.

[52] D.E. Lansky, B. Mandimutsira, B. Ramdhanie, M. Clausen, J. Penner-Hahn, S.A. Zvyagin, J. Telser, J. Krzystek, R. Zhan, Z. Ou, K.M. Kadish, L. Zakharov, A.L. Rheingold, D.P. Goldberg, Inorg. Chem. 44 (2005) 4485.

[53] T. Katsuki, Adv. Synth. Catal. 344 (2002) 131.

[54] H. Jacobsen, L. Cavallo, Chem.: Eur. J. 7 (2001) 800.

[55] T. Flessner, S. Doye, Journal Fur Praktische Chemie-Chemiker-Zeitung 341 (1999) 436.

[56] Y.N. Ito, T. Katsuki, Bull. Chem. Soc. Jpn. 72 (1999) 603.

[57] C.T. Dalton, K.M. Ryan, V.M. Wall, C. Bousquet, D.G. Gilheany, Topics Catal. 5 (1998) 75.

[58] T. Katsuki, J. Mol. Catal.: Chem. 113 (1996) 87.

[59] T. Katsuki, Coord. Chem. Rev. 140 (1995) 189.

[60] W. Adam, C. Mock-Knoblauch, C.R. Saha-Moller, M.J. Herderich, Am. Chem. Soc. 122 (2000) 9685.

[61] L. Cavallo, H. Jacobsen, Angew. Chem. Int. Ed. Engl. 39 (2000) 589.

[62] T. Strassner, K.N. Houk, Org. Lett. 1 (1999) 419.

[63] C. Linde, B. Akermark, P.O. Norrby, M.J. Svensson, Am. Chem. Soc. 121 (1999) 5083.

[64] T. Linker, Angew. Chem. Int. Ed. Engl. 36 (1997) 2060.

[65] K.A. Jorgensen, Chem. Rev. 89 (1989) 431.

[66] M.P. Feth, C. Bolm, J.P. Hildebrand, M. Köhler, O. Beckmann, M. Bauer, R. Ramamonjisoa, H. Bertagnolli, Chem. Eur. J. 9 (2003) 1348.

[67] M. Palucki, N.S. Finney, P.J. Pospisil, M.L. Guler, T. Ishida, E.N. Jacobsen, J. Am. Chem. Soc. 120 (1998) 948.

[68] N.S. Finney, P.J. Pospisil, S. Chang, M. Palucki, R.G. Konsler, K.B. Hansen, E.N. Jacobsen, Angew. Chem. Int. Ed. Engl. 36 (1997) 1720.

[69] D. Schroder, S. Shaik, H. Schwarz, Acc. Chem. Res. 33 (2000) 139.

[70] D.A. Plattner, Angew. Chem. Int. Ed. Engl. 38 (1999) 82.

[71] S. Shaik, M. Filatov, D. Schroder, H. Schwarz, Chem.: Eur. J. 4 (1998) 193.

[72] C. Linde, M. Arnold, P.O. Norrby, B. Akermark, Angew. Chem. Int. Ed. Engl. 36 (1997) 1723.

[73] T. Hamada, T. Fukuda, H. Imanishi, T. Katsuki, Tetrahedron 52 (1996) 515.

[74] J.A. Smegal, B.C. Schardt, C.L. Hill, J. Am. Chem. Soc. 105 (1983) 3510.

[75] D. Feichtinger, D.A. Plattner, Chem.: Eur. J. 7 (2001) 591.

[76] D. Feichtinger, D.A. Plattner, Angew. Chem. Int. Ed. Engl. 36 (1997) 1718.

[77] J.T. Groves, M.K. Stern, J. Am. Chem. Soc. 110 (1988) 8628.

[78] W.J. Song, M.S. Seo, S. DeBeer-George, T. Ohta, R. Song, M.-J. Kang, T. Tosha, T. Kitagawa, E.I. Solomon, W.J. Nam, Am. Chem. Soc. 129 (2007) 1268.

[79] T.H. Parsell, R.K. Behan, M.T. Green, M.P. Hendrich, A.S. Borovik, J. Am. Chem. Soc. 128 (2006) 8728.

[80] R. Gupta, C.E. MacBeth, V.G. Young, A.S. Borovik, J. Am. Chem. Soc. 124 (2002) 1136.

[81] M.T. Caudle, V.L. Pecoraro, J. Am. Chem. Soc. 119 (1997) 3415.

[82] R.S. Czernuszewicz, Y.O. Su, M.K. Stern, K.A. Macor, D. Kim, J.T. Groves, T.G. Spiro, J. Am. Chem. Soc. 110 (1988) 4158.

[83] P. Tarte, Spectrochim. Acta 13 (1958) 107.

[84] P.A. Bulliner, T.G. Spiro, Inorg. Chem. 8 (1969) 1023.

[85] J.Y. Yang, J. Bachmann, D.G. Nocera, J. Org. Chem. 71 (2006) 8706.

[86] S.-Y. Liu, D.G. Nocera, J. Am. Chem. Soc. 127 (2005) 5278.

[87] S.-Y. Liu, J.D. Soper, J.Y. Yang, E.V. Rybak-Akimova, D.G. Nocera, Inorg. Chem. 45 (2006) 7572.

[88] S.-Y. Liu, D.G. Nocera, Tetrahedron Lett. 47 (2006) 1923.

[89] N.A. Law, M.T. Caudle, V.L. Pecoraro, in: Advances in Inorganic Chemistry, vol. 46, 1999, p. 305.

[90] K. Ghosh, A.A. Eroy-Reveles, M.M. Olmstead, P.K. Mascharak, Inorg. Chem. 44 (2005) 8469.

[91] H. Chen, J.W. Faller, R.H. Crabtree, G.W. Brudvig, J. Am. Chem. Soc. 126 (2004) 7345.

[92] H.Y. Chen, M.-N. Collomb, C. Duboc, G. Blondin, E. Riviere, J.W. Faller, R.H. Crabtree, G.W. Brudvig, Inorg. Chem. 44 (2005) 9567.

[93] N. Kitajima, M. Osawa, M. Tanaka, Y. Moro-oka, J. Am. Chem. Soc. 113 (1991) 8952.

[94] M. Lundberg, M.R.A. Blomberg, P.E.M. Siegbahn, Inorg. Chem. 43 (2004) 264.

[95] M. Lundberg, P.E.M. Siegbahn, Phys. Chem. Chem. Phys. 6 (2004) 4772.

[96] M. Osawa, M. Tanaka, K. Fujisawa, N. Kitajima, Y. Moro-oka, Chem. Lett. (1996) 397.

[97] E. Larson, M.S. Lah, X.H. Li, J.A. Bonadies, V.L. Pecoraro, Inorg. Chem. 31 (1992) 373.

[98] N. Kitajima, U.P. Singh, H. Amagai, M. Osawa, Y. Moro-oka, J. Am. Chem. Soc. 113 (1991) 7757.

[99] E.J. Larson, V.L. Pecoraro, J. Am. Chem. Soc. 113 (1991) 3810.

[100] C.A. McAuliffe, R.V. Parish, S.M. Abu-El-Wafa, R.M. Issa, Inorg. Chim. Acta 115 (1986) 91.

[101] M.K. Chan, W.H. Armstrong, J. Am. Chem. Soc. 113 (1991) 5055.

[102] L.J. Boucher, C.G. Coe, Inorg. Chem. 15 (1976) 1334.

[103] M.J. Baldwin, T.L. Stemmler, P.J. Riggs-Gelasco, M.L. Kirk, J.E. Penner-Hahn, V.L. Pecoraro, J. Am. Chem. Soc. 116 (1994) 11349.

[104] M.T. Caudle, P. Riggs-Gelasco, A.K. Gelasco, J.E. Penner-Hahn, V.L. Pecoraro, Inorg. Chem. 35 (1996) 3577.

[105] P.M. Plaksin, R.C. Stoufer, M. Mathew, G.J. Palenik, J. Am. Chem. Soc. 94 (1972) 2121.

[106] S.R. Cooper, M. Calvin, J. Am. Chem. Soc. 99 (1977) 6623.

[107] S.R. Cooper, G.C. Dismukes, M.P. Klein, M. Calvin, J. Am. Chem. Soc. 100 (1978) 7248.

[108] R. Manchanda, G.W. Brudvig, R.H. Crabtree, J.E. Sarneski, M. Didiuk, Inorg. Chim. Acta 212 (1993) 135.

[109] G.C. Dismukes, J.E. Sheats, J.A. Smegal, J. Am. Chem. Soc. 109 (1987) 7202.

[110] G.C. Dismukes, K. Ferris, P. Watnick, Photobiochem. Photobiophys. 3 (1982) 243.

[111] G.C. Dismukes, Y. Siderer, Proc. Natl. Acad. Sci. U.S.A.: Biol. Sci. 78 (1981) 274.

[112] X. Tang, B. Diner, B. Larsen, M. Gilchrist Jr, G. Lorigan, R. Britt, PNAS 91 (1994) 704.

[113] D.W. Randall, B.E. Sturgeon, J.A. Ball, G.A. Lorigan, M.K. Chan, M.P. Klein, W.H. Armstrong, R.D. Britt, J. Am. Chem. Soc. 117 (1995) 11780.

[114] J.M. Peloquin, R.D. Britt, Biochim. Biophys. Acta (BBA): Bioenerg. 1503 (2001) 96.

[115] D.W. Randall, A. Gelasco, M.T. Caudle, V.L. Pecoraro, R.D. Britt, J. Am. Chem. Soc. 119 (1997) 4481.

[116] P.A. Goodson, J. Glerup, D.J. Hodgson, K. Michelsen, E. Pedersen, Inorg. Chem. 29 (1990) 503.

[117] A.K. Poulsen, A. Rompel, C. McKenzie, J. Angew. Chem. Int. Ed. Engl. 44 (2005) 6916.

[118] S. Mukhopadhyay, W.H. Armstrong, J. Am. Chem. Soc. 125 (2003) 13010.

[119] J.H.A. Nugent, D.J. Maclachlan, S.E.J. Rigby, M.C.W. Evans, Photosynth. Res. 38 (1993) 341.

[120] D.J. Maclachlan, B.J. Hallahan, S.V. Ruffle, J.H.A. Nugent, M.C.W. Evans, R.W. Strange, S.S. Hasnain, Biochem. J. 285 (1992) 569.

[121] J.E. Penner-Hahn, R.M. Fronko, V.L. Pecoraro, C.F. Yocum, S.D. Betts, N.R. Bowlby, J. Am. Chem. Soc. 112 (1990) 2549.

[122] K. Wieghardt, U. Bossek, B. Nuber, J. Weiss, J. Bonvoisin, M. Corbella, S.E. Vitols, J.J. Girerd, J. Am. Chem. Soc. 110 (1988) 7398.

[123] S. Pal, W.H. Armstrong, Inorg. Chem. 31 (1992) 5417.

[124] U. Bossek, T. Weyhermüller, K. Wieghardt, B. Nuber, J. Weiss, J. Am. Chem. Soc. 112 (1990) 6387.

[125] K. Wieghardt, U. Bossek, J. Bonvoisin, P. Beauvillain, J.-J. Girerd, B. Nuber, J. Weiss, J. Heinze, Angew. Chem. Int. Ed. Engl. 25 (1986) 1030.

[126] K. Wieghardt, U. Bossek, D. Ventur, J. Weiss, J. Chem. Soc. Chem. Commun. (1985) 347.

[127] J.E. Sheats, R.S. Czernuszewicz, G.C. Dismukes, A.L. Rheingold, V. Petrouleas, J. Stubbe, W.H. Armstrong, R.H. Beer, S.J. Lippard, J. Am. Chem. Soc. 109 (1987) 1435.

[128] J.A. Kirby, A.S. Robertson, J.P. Smith, A.C. Thompson, S.R. Cooper, M.P. Klein, J. Am. Chem. Soc. 103 (1981) 5529.

[129] V.K. Yachandra, R.D. Guiles, A. McDermott, R.D. Britt, J. Cole, S.L. Dexheimer, K. Sauer, M.P. Klein, J. Phys. Colloq. C8 (1986) 2.

[130] J.L. Cole, V.K. Yachandra, A.E. McDermott, R.D. Guiles, R.D. Britt, S.L. Dexheimer, K. Sauer, M.P. Klein, Biochemistry 26 (1987) 5967.

[131] V.K. Yachandra, R.D. Guiles, A.E. McDermott, J.L. Cole, R.D. Britt, S.L. Dexheimer, K. Sauer, M.P. Klein, Biochemistry 26 (1987) 5974.

[132] J. Cole, V.K. Yachandra, R.D. Guiles, A.E. McDermott, R.D. Britt, S.L. Dexheimer, K. Sauer, M.P. Klein, Biochim. Biophys. Acta 890 (1987) 395.

[133] L.J. Boucher, C.G. Coe, Inorg. Chem. 14 (1975) 1289.

[134] E.J. Larson, V.L. Pecoraro, J. Am. Chem. Soc. 113 (1991) 7809.

[135] J.W. Gohdes, W.H. Armstrong, Inorg. Chem. 31 (1992) 368.

[136] V.K. Yachandra, V.J. Derose, M.J. Latimer, I. Mukerji, K. Sauer, M.P. Klein, Science 260 (1993) 675.

[137] W.B. Tolman, Acc. Chem. Res. 30 (1997) 227.

[138] V.L. Pecoraro, W.Y. Hsieh, Inorg. Chem., submitted for publication.

[139] J.M. Peloquin, K.A. Campbell, D.W. Randall, M.A. Evanchik, V.L. Pecoraro, W.H. Armstrong, R.D. Britt, J. Am. Chem. Soc. 122 (2000) 10926.

[140] K. Sauer, J. Yano, V.K. Yachandra, Photosynth. Res. 85 (2005) 73.

[141] J.L. Casey, K. Sauer, Biochim. Biophys. Acta (BBA): Bioenerg. 767 (1984) 21.

[142] J.C. De Paula, W.F. Beck, G.W. Brudvig, J. Am. Chem. Soc. 108 (1986) 4002.

[143] V.L. Pecoraro, M.J. Baldwin, M.T. Caudle, W.Y. Hsieh, N.A. Law, Pure Appl. Chem. 70 (1998) 925.

[144] E. Larson, A. Haddy, M.L. Kirk, R.H. Sands, W.E. Hatfield, V.L. Pecoraro, J. Am. Chem. Soc. 114 (1992) 6263.

[145] A. Gelasco, V.L. Pecoraro, J. Am. Chem. Soc. 115 (1993) 7928.

[146] A. Gelasco, S. Bensiek, V.L. Pecoraro, Inorg. Chem. 37 (1998) 3301.

[147] W.Y. Hsieh, K.A. Campbell, W. Gregor, R.D. Britt, D.W. Yoder, J.E. Penner-Hahn, V.L. Pecoraro, Biochim. Biophys. Acta: Bioenerg. 1655 (2004) 149.

[148] K.A. Campbell, J.M. Peloquin, D.P. Pham, R.J. Debus, R.D. Britt, J. Am. Chem. Soc. 120 (1998) 447.

[149] W.F. Beck, G.W. Brudvig, Biophys. J. 49 (1986) A485.

[150] M.T. Caudle, J.W. Kampf, M.L. Kirk, P.G. Rasmussen, V.L. Pecoraro, J. Am. Chem. Soc. 119 (1997) 9297.

[151] T.M. Rajendiran, M.L. Kirk, I.A. Setyawati, M.T. Caudle, J.W. Kampf, V.L. Pecoraro, Chem. Commun. (2003) 824.

[152] J. Limburg, J.S. Vrettos, L.M. Liable-Sands, A.L. Rheingold, R.H. Crabtree, G.W. Brudvig, Science 283 (1999) 1524.

[153] C. Baffert, S. Romain, A. Richardot, J.C. Lepretre, B. Lefebvre, A. Deronzier, M.N. Collomb, J. Am. Chem. Soc. 127 (2005) 13694.

[154] C. Baffert, M.N. Collomb, A. Deronzier, J. Pecaut, J. Limburg, R.H. Crabtree, G.W. Brudvig, Inorg. Chem. 41 (2002) 1404.

[155] C. Baffert, H.G. Chen, R.H. Crabtree, G.W. Brudvig, M.N. Collomb, J. Electroanal. Chem. 506 (2001) 99.

[156] M.-N. Collomb, A. Deronzier, A. Richardot, J. Pecaut, New J. Chem. 23 (1999) 351.

[157] K. Narita, T. Kuwabara, K. Sone, K.I. Shimizu, M. Yagi, J. Phys. Chem. B 110 (2006) 23107.

[158] J. Limburg, J.S. Vrettos, M.N. Collomb, L.M. Liable-Sands, A.L. Rheingold, R.H. Crabtree, G.W. Brudvig, J. Inorg. Biochem. 74 (1999) 207.

[159] V.K. Yachandra, K. Sauer, M.P. Klein, Chem. Rev. 96 (1996) 2927.

[160] T.G. Carrell, S. Cohen, G.C. Dismukes, J. Mol. Catal. A: Chem. 187 (2002) 3.

[161] Y. Shimazaki, T. Nagano, H. Takesue, B.H. Ye, F. Tani, Y. Naruta, Angew. Chem. Int. Ed. Engl. 43 (2004) 98.

[162] B. Meunier, Chem. Rev. 92 (1992) 1411.

[163] Y. Watanabe, H. Fujii, in: Metal-Oxo and Metal-Peroxo Species in Catalytic Oxidations, vol. 97, 2000, p. 61.

[164] R. Zhang, J.H. Horner, M.J. Newcomb, Am. Chem. Soc. 127 (2005) 6573.

[165] R. Lomoth, A. Magnuson, M. Sjõdin, P. Huang, S. Styring, L. Hammarstrom, Photosynth. Res. 87 (2006) 25.

[166] G. Eilers, C. Zettersten, L. Nyholm, L. Hammarstrom, R. Lomoth, Dalton Trans. (2005) 1033.

[167] P. Huang, A. Magnuson, R. Lomoth, M. Abrahamsson, M. Tamm, L. Sun, B. van Rotterdam, J. Park, L. Hammarstrom, B. Akermark, S. Styring, J. Inorg. Biochem. 91 (2002) 159.

[168] S. Romain, J.-C. Lepretre, J. Chauvin, A. Deronzier, M.-N. Collomb, Inorg. Chem. 46 (2007) 2735.

[169] S. Romain, C. Baffert, S. Dumas, J. Chauvin, J.C. Lepretre, D. Daveloose, A. Deronzier, M.N. Collomb, Dalton Trans. (2006) 5691.

[170] F.A. Cotton, C.A. Murillo, M. Bochmann, Advanced Inorganic Chemistry, 6th ed., Wiley–Interscience, 1999.

[171] R. Bhula, G.J. Gainsford, D.C. Weatherburn, J. Am. Chem. Soc. 110 (1988) 7550.

[172] X.H. Li, D.P. Kessissoglou, M.L. Kirk, C.J. Bender, V.L. Pecoraro, Inorg. Chem. 27 (1988) 1.

[173] D.P. Kessissoglou, M.L. Kirk, C.A. Bender, M.S. Lah, V.L. Pecoraro, J. Chem. Soc. Chem. Commun. (1989) 84.

[174] D.P. Kessissoglou, M.L. Kirk, M.S. Lah, X.H. Li, C. Raptopoulou, W.E. Hatfield, V.L. Pecoraro, Inorg. Chem. 31 (1992) 5424.

[175] A. Yoshino, T. Miyagi, E. Asato, M. Mikuriya, Y. Sakata, K. Sugiura, K. Iwasaki, S. Hino, D. Hino, Chem. Commun. (2000) 1475.

[176] V. Tangoulis, D.A. Malamatari, G.A. Spyroulias, C.P. Raptopoulou, A. Terzis, D.P. Kessissoglou, Inorg. Chem. 39 (2000) 2621.

[177] P. Basu, S. Pal, A. Chakravorty, Inorg. Chem. 27 (1988) 1848.

[178] J.A. Bonadies, M.L. Kirk, M.S. Lah, D.P. Kessissoglou, W.E. Hatfield, V.L. Pecoraro, Inorg. Chem. 28 (1989) 2037.

[179] J. Messinger, J.H.A. Nugent, M.C.W. Evans, Biochemistry 36 (1997) 11055.

[180] J. Messinger, J.H. Robblee, W.O. Yu, K. Sauer, V.K. Yachandra, M.P. Klein, J. Am. Chem. Soc. 119 (1997) 11349.

[181] K.A. Åhrling, S. Peterson, S. Styring, Biochemistry 36 (1997) 13148.

[182] T.A. Roelofs, W.C. Liang, M.J. Latimer, R.M. Cinco, A. Rompel, J.C. Andrews, K. Sauer, V.K. Yachandra, M.P. Klein, Proc. Natl. Acad. Sci. U.S.A. 93 (1996) 3335.

[183] C. Mukherjee, T. Weyhermueller, K. Wieghardt, P. Chaudhuri, Dalton Trans. (2006) 2169.

[184] M.K. Chan, W.H. Armstrong, J. Am. Chem. Soc. 112 (1990) 4985.

[185] S. Kokatam, T. Weyhermuller, E. Bothe, P. Chaudhuri, K. Wieghardt, Inorg. Chem. 44 (2005) 3709.

[186] S. Mukherjee, T. Weyhermuller, E. Bothe, K. Wieghardt, P. Chaudhuri, Dalton Trans. (2004) 3842.

[187] S. Mukherjee, T. Weyhermuller, K. Wieghardt, P. Chaudhuri, Dalton Trans. (2003) 3483.

[188] S. Mukherjee, E. Rentschler, T. Weyhermuller, K. Wieghardt, P. Chaudhuri, Chem. Commun. (2003) 1828.

[189] H.P. Chun, P. Chaudhuri, T. Weyhermuller, K. Wieghardt, Inorg. Chem. 41 (2002) 790.

[190] H. Chun, C.N. Verani, P. Chaudhuri, E. Bothe, E. Bill, T. Weyhermuller, K. Wieghardt, Inorg. Chem. 40 (2001) 4157.

[191] C.N. Verani, S. Gallert, E. Bill, T. Weyhermuller, K. Wieghardt, P. Chaudhuri, Chem. Commun. (1999) 1747.

[192] P. Chaudhuri, C.N. Verani, E. Bill, E. Bothe, T. Weyhermuller, K. Wieghardt, J. Am. Chem. Soc. 123 (2001) 2213.

[193] M. Alexiou, C.M. Zaleski, C. Dendrinou-Samara, J. Kampf, D.P. Kessissoglou, V.L. Pecoraro, Z. Anorg. Allg. Chem. 629 (2003) 2348.

[194] M. Alexiou, C. Dendrinou-Samara, A. Karagianni, S. Biswas, C.M. Zaleski, J. Kampf, D. Yoder, J.E. Penner-Hahn, V.L. Pecoraro, D.P. Kessissoglou, Inorg. Chem. 42 (2003) 2185.

[195] K. Wieghardt, U. Bossek, B. Nuber, J. Weiss, S. Gehring, W. Haase, J. Chem. Soc. Chem. Commun. (1988) 1145.

[196] S. Bhaduri, M. Pink, G. Christou, Chem. Commun. (2002) 2352.

[197] S. Brooker, V. McKee, J. Chem. Soc. Chem. Commun. (1989) 619.

[198] S. Brooker, V. McKee, T. Metcalfe, Inorg. Chim. Acta 246 (1996) 171.

[199] A. Gelasco, A. Askenas, V.L. Pecoraro, Inorg. Chem. 35 (1996) 1419.

[200] K. Wieghardt, U. Bossek, W. Gebert, Angew. Chem. -Int. Ed. Engl. 22 (1983) 328.

[201] T.H. Bennur, D. Srinivas, S. Sivasanker, V.G. Puranik, J. Mol. Catal.: Chem. 219 (2004) 209.

[202] L. Zhang, S.P. Yan, C.H. Li, D.Z. Liao, Z.H. Jiang, P. Cheng, G.L. Wang, L.H. Weng, X.B. Leng, J. Chem. Crystallogr. 30 (2000) 251.

[203] K.S. Hagen, T.D. Westmoreland, M.J. Scott, W.H. Armstrong, J. Am. Chem. Soc. 111 (1989) 1907.

[204] C.E. Dube, S. Mukhopadhyay, P.J. Bonitatebus, R.J. Staples, W.H. Armstrong, Inorg. Chem. 44 (2005) 5161.

[205] M.K. Chan, W.H. Armstrong, J. Am. Chem. Soc. 111 (1989) 9121.

[206] T. Afrati, C. Dendrinou-Samara, C.P. Raptopoulou, A. Terzis, V. Tangoulis, D.P. Kessissoglou, Angew. Chem. Int. Ed. 41 (2002) 2148.

[207] C.W. Zaleski, C. Dendrinou-Samara, M. Alexiou, P. Kanakaraki, J.W. Kampf, J.E. Penner-Hahn, V.L. Pecoraro, D.P. Kessissoglou, in preparation.

[208] S.Y. Wang, K. Folting, W.E. Streib, E.A. Schmitt, J.K. McCusker, D.N. Hendrickson, G. Christou, Angew. Chem. Int. Ed. Engl. 30 (1991) 305.

[209] J.S. Bashkin, H.R. Chang, W.E. Streib, J.C. Huffman, D.N. Hendrickson, G. Christou, J. Am. Chem. Soc. 109 (1987) 6502.

[210] D.N. Hendrickson, G. Christou, E.A. Schmitt, E. Libby, J.S. Bashkin, S.Y. Wang, H.L. Tsai, J.B. Vincent, P.D.W. Boyd, J.C. Huffman, K. Folting, Q.Y. Li, W.E. Streib, J. Am. Chem. Soc. 114 (1992) 2455.

[211] M. Zheng, G.C. Dismukes, Inorg. Chem. 35 (1996) 3307.

[212] G. Blondin, R. Davydov, C. Philouze, M.F. Charlot, S. Styring, B. Akermark, J.J. Girerd, A. Boussac, J. Chem. Soc., Dalton Trans. (1997) 4069.

[213] W.F. Ruettinger, C. Campana, G.C. Dismukes, J. Am. Chem. Soc. 119 (1997) 6670.

[214] W. Ruettinger, M. Yagi, K. Wolf, S. Bernasek, G.C. Dismukes, J. Am. Chem. Soc. 122 (2000) 10353.

[215] W.F. Ruettinger, G.C. Dismukes, Inorg. Chem. 39 (2000) 1021.

[216] T.G. Carrell, A.M. Tyryshkin, G.C. Dismukes, J. Biol. Inorg. Chem. 7 (2002) 2.

[217] J.-Z. Wu, F. De Angelis, T.G. Carrell, G.P.A. Yap, J. Sheats, R. Car, G.C. Dismukes, Inorg. Chem. 45 (2006) 189.

[218] S.Y. Wang, J.C. Huffman, K. Folting, W.E. Streib, E.B. Lobkovsky, G. Christou, Angew. Chem. Int. Ed. Engl. 30 (1991) 1672.

[219] C. Philouze, G. Blondin, S. Ménage, N. Auger, J.-J. Girerd, D. Vigner, M. Lance, M. Nierlich, Angew. Chem. Int. Ed. Engl. 31 (1992) 1629.

[220] S. Styring, A.W. Rutherford, Biochemistry 26 (1987) 2401.

[221] T. Kuntzleman, C.F. Yocum, Biochemistry 44 (2005) 2129.

[222] A. Messerschmidt, A. Rossi, R. Ladenstein, R. Huber, M. Bolognesi, G. Gatti, A. Marchesini, R. Petruzzelli, A. Finazzi-Agro, J. Mol. Biol. 206 (1989) 513.

[223] J. Limburg, V.A. Szalai, G.W. Brudvig, J. Chem. Soc., Dalton Trans. (1999) 1353.

[224] J.S. Vrettos, J. Limburg, G.W. Brudvig, Biochim. Biophys. Acta: Bioenerg. 1503 (2001) 229.

[225] J.S. Vrettos, G.W. Brudvig, Philos. Trans. R. Soc. Lond. B 357 (2002) 1395.

[226] C.W. Hoganson, G.T. Babcock, Science 277 (1997) 1953.

[227] M. Haumann, P. Liebisch, C. Muller, M. Barra, M. Grabolle, H. Dau, Science 310 (2005) 1019.